

# Trends analysis of PM source contributions and chemical tracers in NE Spain during 2004 - 2014:

## A multi-exponential approach.

Marco Pandolfi <sup>1,\*</sup>, Andrés Alastuey <sup>1</sup>, Noemi Pérez <sup>1</sup>, Cristina Reche <sup>1</sup>, Iria Castro <sup>1</sup>, Victor Shatalov <sup>2</sup> and Xavier Querol <sup>1</sup>

<sup>1</sup> Institute of Environmental Assessment and Water Research, c/ Jordi-Girona 18-26, 08034 Barcelona, Spain

<sup>2</sup> Meteorological Synthesizing Centre – East, 2nd Roshchinsky proezd, 8/5, 115419 Moscow, Russia

\*Corresponding author: marco.pandolfi@idaea.csic.es

## Abstract

In this work for the first time data from two twin stations (Barcelona, urban background, and Montseny, regional background), located in NE of Spain, were used to study the trends of the concentrations of different chemical species in PM<sub>10</sub> and PM<sub>2.5</sub> along with the trends of the PM<sub>10</sub> source contributions from Positive Matrix Factorization (PMF) model. Eleven years of chemical data (2004–2014) were used for this study. Trends of both specie concentrations and source contributions were studied using the Mann-Kendall test for linear trends and a new approach based on multi-exponential fit of the data. Despite the fact that different PM fractions (PM<sub>2.5</sub>, PM<sub>10</sub>) showed linear decreasing trends at both stations, the contributions of specific sources of pollutants and the related chemical tracers showed exponential decreasing trends. The different types of trends observed reflected the different effectiveness and/or time of implementation of the measures taken to reduce the concentrations of atmospheric pollutants. Moreover, the trends of the contributions from specific sources such as those related with industrial activities and with primary energy consumption mirrored the effect of the financial crisis in Spain from 2008. The sources that showed statistically significant downward trends at both Barcelona (BCN) and Montseny (MSY) during 2004-2014 were *Secondary sulfate*, *Secondary nitrate*, and *V-Ni bearing* source. The contributions from these sources decreased exponentially during the considered period indicating that the observed decrease was not gradual and consistent over time. Conversely, the decreasing trend was less steep at the end of the period compared to the beginning thus likely indicating the attainment of a lower limit. Moreover, statistically significant decreasing trends were observed for the contributions to PM from the *Industrial/Traffic* source at MSY (mixed metallurgy and road traffic) and from the *Industrial* (metallurgy mainly) source at BCN. These sources were clearly linked with anthropogenic activities and the observed decreasing trends confirmed the effectiveness of pollution control measures implemented at EU or regional/local levels. Conversely, the contributions from sources mostly linked with natural processes such as *Aged Marine* and *Aged Organics* did not show statistically significant trends. The general trends observed for the calculated PMF source contributions well reflected the trends observed for the chemical tracers of these pollutant sources.

## 1. Introduction

35 Meeting the air quality (AQ) standards is one of the major environmental objectives to protect people from  
36 breathing air with high levels of pollution. Many studies have been published in these last years showing clearly  
37 that the concentrations of particulate matter (PM), and other air pollutants such as sulphur dioxide (SO<sub>2</sub>) and  
38 carbon monoxide (CO), have markedly decreased during the last 15 years in many European Countries (EEA, 2013;  
39 Barmpadimos et al., 2012; Cusack et al., 2012; Querol et al., 2014; Guerreiro et al., 2014 among others). Cusack  
40 et al. (2012) reported the reduction in PM<sub>2.5</sub> concentrations observed at regional background (RB) stations in  
41 Spain and across Europe, and, in most cases, the observed reduction was gradual and consistent over time,  
42 implying the success of cleaner anthropogenic activities. Barmpadimos et al. (2012) have also shown that PM<sub>10</sub>  
43 concentrations decreased at a number of urban background (UB) and rural background stations in five European  
44 countries. Henschel et al. (2013) reported the dramatic decrease in SO<sub>2</sub> levels across six European cities, reflecting  
45 the reduction in sulphur content in fuels, as part of EU legislation, coupled with the shift towards the use of  
46 cleaner fuels. EEA (2013) also reported general decreases in NO<sub>2</sub> concentrations even if lower compared to PM.  
47 However, Henschel et al. (2015) showed that the NO<sub>x</sub> concentrations at traffic sites in many EU cities remained  
48 unchanged underlining the need of further regulative measures to meet the air quality standards for this  
49 pollutant. In fact an important proportion of the European population lives in areas exceeding the AQ standards  
50 for the annual limit value of NO<sub>2</sub>, the daily limit value of PM<sub>10</sub> and the health protection objective of O<sub>3</sub> (EEA,  
51 2013; 2015). PM<sub>10</sub> and NO<sub>2</sub> are still exceeded mostly in urban areas, and especially at traffic sites (Harrison et al.,  
52 2008; Williams and Carslaw, 2011; EEA, 2013; among others). In Spain for example it has been reported that more  
53 than 90% of the NO<sub>2</sub> exceedances are attributed to road traffic emissions (Querol et al., 2012). Guerreiro et al.  
54 (2014) furthermore evidenced notable reduction of ambient air concentration of SO<sub>2</sub>, CO and Pb using data  
55 available in Airbase (EEA, 2013) and covering 38 European countries. Querol et al. (2014) reported trends for 73  
56 measurement sites across Spain including RB, UB, traffic stations (TS) and Industrial sites (IND). They observed  
57 marked downward concentration trends for PM<sub>10</sub>, PM<sub>2.5</sub>, CO and SO<sub>2</sub> at most of the RB, UB, TR and IND sites  
58 considered. Similarly, Salvador et al. (2012) detected statistically significant downward trends in the  
59 concentrations of SO<sub>2</sub>, NO<sub>x</sub>, CO and PM<sub>2.5</sub> at most of the urban and urban-background monitoring sites in the  
60 Madrid metropolitan area during 1999-2008. Cusack et al. (2012) and Querol et al. (2014) have also shown the  
61 highly statistically significant decreasing trends observed at regional level in NE Spain for many trace elements  
62 since 2002 (Pb, Cu, Zn, Mn, Cd, As, Sn, V, Ni, Cr).

63 The observed reduction of air pollutants across Europe is the results of efficient emission abatement strategies  
64 as for example those implemented in the Industrial Emission Directives (IPPC Integrated Pollution Prevention and  
65 Control and subsequent Industrial Emission Directives 1996/61/EC and 2008/1/EC), the Large Combustion Plants  
66 Directive (LCPD; 2001/80/EC), the EURO standards on road traffic emission (1998/69/EC, 2002/80/EC,  
67 2007/715/EC), the IMO (International Maritime Organization) directive on sulfur content in fuel and SO<sub>x</sub> and NO<sub>x</sub>  
68 emissions from ships (IMO, 2011; Directive 2005/33/EC). Additionally, the financial crisis, causing mainly a  
69 reduction of the primary energy consumption from 2008-2009, contributed to the decrease of the ambient  
70 concentration of pollutants observed in Spain (Querol et al., 2014).

71 Moreover, national and regional measures for AQ have been taken in many European Countries. In Spain a  
72 national AQ plan was approved in 2011 and updated in 2013 by the Council of Ministers of the Government of  
73 Spain. Furthermore, 45 regional and 3 local (city scale) AQ plans have been implemented since 2004 in Spain.  
74 These AQ Plans mostly focused on improving AQ at major city centers or specific industrial areas.

75 Thanks to the aforementioned measures, there is clear evidence that the concentrations of PM in many European  
76 countries have markedly decreased during the last decades. However, in spite of the above policy efforts, a  
77 significant proportion of the urban population in Europe lives in areas exceeding the World Health Organisation  
78 (WHO) air quality (AQ) standards i.e. for  $PM_{2.5}$ ,  $PM_{10}$  and ozone (EEA, 2013, 2015).

79 Trend analysis of the concentration of air pollutants helps in evaluating the effectiveness of specific AQ measures  
80 depending on the pollutant considered. Examining data over time also makes it possible to predict future  
81 frequencies and/or rates of occurrence making future projections. For the abovementioned reasons, it is  
82 especially attractive the feasibility of studying the trends of the contributions to PM mass from specific pollutant  
83 sources along with the trends of the chemical tracers of these sources.

84 For what we are concerned in the majority of studies dealing with trend analysis, linear fits were applied for  
85 example by using Mann-Kendall or Theil-Sen methods (Theil, 1950; Sen, 1968), the latter being available for  
86 example in the Openair software (Carslaw, 2012; Carslaw and Ropkins, 2012). However, linear fit of data does not  
87 always properly represent the observed trends. As we will show, different abatement strategies and periods of  
88 implementation may change from one pollutant to another thus leading to different trends for different  
89 pollutants, even over the same period. Thus, non-linear fit of the data may be at times strongly recommended.

90 The main aim of this work was to study the trends of source contributions to  $PM_{10}$  and specific chemical species  
91 in both  $PM_{10}$  and  $PM_{2.5}$  using both the consensus methodology for linear fit of the data (Mann-Kendall) and a non-  
92 linear approach. The data of Spanish national emissions and energy consumption are also evaluated to interpret  
93 the observed trends. Understanding past trends may be relevant for devising new strategies for air pollution  
94 abatement. PM chemical speciated data collected from 2004 to 2014 at regional (Montseny; NE Spain) and urban  
95 (Barcelona, NE Spain) sites were used with this aim. The selected period allowed for trend analysis at these twin  
96 stations over a common period. The Positive Matrix Factorization (PMF) model was used to apportion ambient  
97  $PM_{10}$  concentrations into pollutant sources. The PMF model, as other Receptor Models (RM), is widely used being  
98 a powerful tool to help policy makers to design more targeted approaches to protecting public health. Thus, the  
99 novelty of this study lies mainly in a) the opportunity to study the trends of pollutant source contributions from  
100 PMF model at two twin stations representative of the urban and regional environments in the Western  
101 Mediterranean, and, b) in the use of a novel non-linear approach for trend studies.

102 **2. Measurement sites and Methodology**

103 **2.1 Measurement sites**

104 The Montseny measurement station (MSY, 41°46'45.63" N, 02°21'28.92" E, 720 m a.s.l.) is a regional background  
105 site in NE of Spain (Figure 1). The MSY station is located within a regional natural park about 50 km to the NNE of  
106 the city of Barcelona (BCN) and 25 km from the Mediterranean coast. This site is representative of the typical  
107 regional background conditions of the Western Mediterranean Basin (WMB) characterized by severe pollution  
108 episodes affecting not only the coastal sites closest to the emission sources, but also the more elevated rural and  
109 remote areas land inwards due to thermally driven winds (i.e. Pérez et al., 2008; Pey et al., 2010; Pandolfi et al.,  
110 2011; 2014). This station is part of ACTRIS ([www.actris.net](http://www.actris.net)) and GAW ([www.wmo.int/gaw](http://www.wmo.int/gaw)) networks, EMEP  
111 (<http://www.emep.int/>) and the measuring network of the Government of Catalonia.

112 The Barcelona measurement station (BCN, 41°23'24.01" N, 02°06'58.06" E, 68 m a.s.l.) is an urban background  
113 measurement site influenced by vehicular emissions from one of the main avenues of the city (Diagonal Avenue)  
114 located at a distance of around 300 m (cf. Fig. 1). The BCN measurement site is part of the Air Quality measuring  
115 network of the Government of Catalonia. The Metropolitan Area of Barcelona (BMA), with nearly 4.5 million  
116 inhabitants, covers an 8 km wide strip between the Mediterranean Sea and the coastal mountain range. Several  
117 industrial zones, power plants, and highways are located in the area, making this region to one of the most  
118 polluted in the WMB (i.e. Querol et al., 2008; Amato et al., 2009; Pandolfi et al., 2012; 2013; 2014). At BCN the  
119 location of the measuring station changed in 2009 when it was moved by around 500 m (cf. Fig. 1). The effect of  
120 this change on PM measurements performed at BCN will discuss later.

121

## 122 **2.2 Real-time and gravimetric PM measurements**

123 Real-time PM concentrations were continuously measured at 1h resolution by optical particle counters (OPC)  
124 using GRIMM spectrometers (GRIMM 180 at MSY, and GRIMM 1107, 1129 and 180 at BCN). Hourly PM  
125 concentrations were corrected by comparison with 24h gravimetric mass measurements of PM<sub>x</sub> (Alastuey et al.,  
126 2011).

127 For gravimetric measurements 24h PM<sub>x</sub> samples were collected at both stations every 3-4 days on 150 mm quartz  
128 micro-fiber filters (Pallflex QAT and Whatman) with a high-volume (Hi-Vol) samplers (DIGITEL DH80 and/or MCV  
129 CAV-A/MSb at 30 m<sup>3</sup>h<sup>-1</sup>). The mass of PM<sub>10</sub> and PM<sub>2.5</sub> samples collected on filters was determined using the EN  
130 12341 and the EN14907 gravimetric procedures, respectively.

131

132

133

### 134 **2.2.1 PM chemical speciated data**

Once the gravimetric mass was determined from filters, the samples were analyzed with different techniques including acidic digestion ( $\frac{1}{2}$  of each filter;  $\text{HNO}_3\text{:HF:HClO}_4$ ), water extraction of soluble anions ( $\frac{1}{4}$  of each filter), and thermal-optical analysis ( $1.5\text{ cm}^2$  sections). Inductively Coupled Atomic Emission Spectrometry, ICP-AES, (IRIS Advantage TJA Solutions, THERMO) was used for the determination of the major elements (Al, Ca, Fe, K, Na, Mg, S, Ti, P), and Inductively Coupled Plasma Mass Spectrometry, ICP-MS, (X Series II, THERMO) for the trace elements (Li, Ti, V, Cr, Mn, Co, Ni, Cu, Zn, As, Se, Rb, Sr, Cd, Sn, Sb, Ba, rare earths, Pb, Bi, Th, U). Ionic Chromatography was used for the concentrations of  $\text{NO}_3^-$ ,  $\text{SO}_4^{2-}$  and  $\text{Cl}^-$ , whereas  $\text{NH}_4^+$  was determined using a specific electrode MODEL 710 A+, THERMO Orion. The levels of OC and EC were determined by a thermal-optical carbon analyzer (SUNSET), using protocol EUSAAR\_2 (Cavalli et al., 2010). Other analytical details may be found in Querol et al. (2008).

Following the above procedures,  $\text{PM}_{10}$  and  $\text{PM}_{2.5}$  chemical speciated data were obtained at MSY for the period 2004-2014 resulting in 1093 and 794 samples, respectively. At BCN  $\text{PM}_{10}$  and  $\text{PM}_{2.5}$  data were obtained during 2004-2014 resulting in 1037 and 1063 samples, respectively.

147

### 2.3 Positive Matrix Factorization (PMF) model.

The PMF model (PMFv5.0, EPA) was used on the collected daily speciated data for source identification and apportionment in  $\text{PM}_{10}$  at both sites. Detailed information about the PMF model can be found in literature (Paatero and Tapper 1994; Paatero 1997; Paatero and Hopke 2003; Paatero et al. 2005). The PMF model is a factor analytical tool reducing the dimension of the input matrix in a limited number of factors (or sources) and it is based on the weighted least-squares method. Thus, most important in PMF applications is the estimation of uncertainties of the chemical species included in the input matrix. In the present study, individual uncertainties and detection limits were calculated as in Escrig et al. (2009) and Amato et al. (2009). Thus, both the analytical uncertainties and the standard deviations of species concentrations in the blank filters were considered in the uncertainties calculations. The signal-to-noise ratio (S/N) was estimated starting from the calculated uncertainties and used as a criteria ( $\text{S/N} > 2$ ) for selecting the species used within the PMF model. In order to avoid any bias in the PMF results, the data matrix was uncensored (Paatero 2004). The PMF was run in robust mode (Paatero 1997), and rotational ambiguity was handled by means of the  $F_{\text{PEAK}}$  parameter (Paatero et al. 2005). The optimal number of sources was selected by inspecting the variation of the objective function  $Q$  (defined as the ratio between residuals and errors in each data value) with varying number of sources (i.e. Paatero et al., 2002) and by studying the physical meaningfulness of the calculated factors.

164

165

### 2.4 Mann-Kendall (MK) fit

167 The purpose of the Mann-Kendall (MK) test (Mann 1945, Kendall 1975, Gilbert 1987) is to statistically assess if  
 168 there is a monotonic upward or downward trend of the variable of interest over time. A monotonic upward  
 169 (downward) trend means that the variable consistently increases (decreases) through time. The Mann-Kendall  
 170 test tests the null hypothesis  $H_0$  of no trend, i.e. the observations are randomly ordered in time, against the  
 171 alternative hypothesis,  $H_1$ , where there is an increasing or decreasing monotonic trend. The main advantage of  
 172 the Mann-Kendall test is that data need not conform to any particular distribution and missing data are allowed.  
 173 To estimate the slope of the trend the Sen's method was used (Salmi et al. 2002).

174

## 175 **2.5 Multi-exponential (ME) fit**

176 A Program aiming at studying trends of time series of air pollution in the multi-exponential form was developed  
 177 within the *The Task Force on Measurements and Modelling* (TFMM) by the *Meteorological Synthesizing Centre –*  
 178 *East* (MSC-E; <http://www.msceast.org/>) group (Shatalov et al., 2015). The TFMM together with the *Task Force on*  
 179 *Emission Inventories and Projections* (TFEIP), the *Task Force on Integrated Assessment Modelling* (TFIAM), and  
 180 *Task Force on Hemispheric Transport of Air Pollution* (TFHTAP) provide a fora for discussion and scientific  
 181 exchange in support of the EMEP (*European Monitoring and Evaluation Programme*; <http://www.emep.int/>) work  
 182 plan which is a scientifically based and policy driven programme under the *Convention on Long-range*  
 183 *Transboundary Air Pollution* (CLRTAP; [http://www.unece.org/env/lrtap/lrtap\\_h1.html](http://www.unece.org/env/lrtap/lrtap_h1.html)) promoting the  
 184 international co-operation to solve transboundary air pollution problems. The TFMM was established in 2000 to  
 185 evaluate measurements and modeling and to further develop working methods and tools. In this context, five  
 186 EMEP Centers are undertaking efforts in support of the EMEP work plan, namely the *MSC-E*, the *Centre on*  
 187 *Emission Inventories and Projections* (CEIP; <http://www.ceip.at/>), the *Chemical Coordinating Centre* (CCC;  
 188 <http://www.nilu.no/projects/ccc/>), the *Meteorological Synthesizing Centre – West* (MSC-W;  
 189 [http://emep.int/mscw/index\\_mscw.html](http://emep.int/mscw/index_mscw.html)), and the *Centre for Integrated Assessment Modelling* (CIAM;  
 190 <http://www.iiasa.ac.at/~rains/ciam.html>). In 2014, the TFMM initiated a dedicated exercise to assess the  
 191 efficiency of air pollution mitigation strategies over the past 20 years to assess the benefit of the CLRTAP main  
 192 policy instrument. Within this exercise a software was made available by EMEP/MSC-E Center aiming at studying  
 193 non-linear trends. Annual, monthly and daily resolution data can be analyzed with the help of this program. Since  
 194 in this paper we will apply the program to annual averages of specie concentrations and source contributions, we  
 195 restrict the description of the multi-exponential approximations for this case. In particular, seasonal variations  
 196 are not included into consideration. The basic equations solved by the program for this particular case (annual  
 197 averages) are reported below:

198

$$199 \quad C_t = a_1 \cdot \exp\left(-\frac{t}{\tau_1}\right) + a_2 \cdot \exp\left(-\frac{t}{\tau_2}\right) + \dots + a_n \cdot \exp\left(-\frac{t}{\tau_n}\right) + \omega_t \quad (1)$$

200

Where,  $C_t$  are the values of the considered time series, with  $t = 1, \dots, N$ ,  $N$  being the length of the series (years),  $\tau_n$  are the characteristic times of the considered exponential,  $a_n$  are constants and  $\omega_t$  are the residue values. In the case of single exponential decay ( $n=1$ ) the characteristic time  $\tau$  is the time at which the pollutant concentration is reduced to  $1/e$  ( $= 0.3678$ ) times its initial value. The main difference between linear and exponential fit is that in the latter case the trend is not gradual and constant over time. For an exponential trend the absolute [ $\mu\text{g}/\text{m}^3$ ] reduction per year decreases with time being the highest at the beginning of the period. Conversely, for a linear fit the absolute reduction is constant over time. For an exponential fit, the lower the characteristic time  $\tau$  the more rapidly the considered quantity vanish. Deviations from single exponential fit can be taken into account introducing more exponential terms. In this work for example two exponential terms were sometime used. In this case, two characteristic times are calculated by the software. If the decrease of the considered quantity is very sharp at the beginning of the period (more than exponential) than both  $\tau_1$  and  $\tau_2$  are positive. Conversely, an exponential term with negative  $\tau$  takes into account for possible increases of the quantity at the end of the period. Both  $\tau_n$  and  $a_n$  are calculated by the program by means of the least square method minimizing the residue  $\omega$  and the statistical significance of the exponential fit is provided by means of the p-value. The number of exponential terms that should be included into the approximation can be evaluated using F-statistics (i.e. Smith, 2002). For example, the F-statistics for the evaluation of the statistical significance of the second term in equation (1) for  $n = 2$  can be calculated as:

218

$$F = \frac{(SS_1 - SS_2)}{2 \cdot s} \quad (2)$$

220

where  $SS_1$  and  $SS_2$  are sums of squares of residual component for approximations with one and two exponential terms, respectively, and  $s$  is the estimate of standard deviation of residual component. This statistics follows approximately the Fisher distribution with 2 and  $N - 2$  degrees of freedom. Second exponential is considered to be significant if  $F$  exceeds the corresponding threshold value at the chosen significance level.

The following parameters can be calculated from equation (1):

$$\text{- Total Reduction (TR): } TR = \frac{(C_{beg} - C_{end})}{C_{beg}} = 1 - \frac{C_{end}}{C_{beg}} \quad (3)$$

$$\text{- Annual reduction for year } i: R_i = \frac{\Delta C_i}{C_i} = 1 - \frac{C_{i+1}}{C_i} \quad (4)$$

$$\text{- Average annual reduction: } R_{av} = 1 - \left( \frac{C_{end}}{C_{beg}} \right)^{\frac{1}{N-1}} \quad (5)$$

Where  $C_{beg}$  and  $C_{end}$  are respectively the first and the last points of the exponential fit. The formula for calculation of average annual reduction takes into account that the ratio  $C_{i+1} / C_i$  is a multiplicative quantity, so that geometrical mean of ratios should be used. The relative contribution of residues (Residual Component: RC) is

232 calculated as the standard deviation of the ratios between the residue values of the fit  $\omega$  (cf. Eq. 1) and the main  
233 component of the fit.

234 The MSC-E also proposed a statistic which measures the deviation of the obtained trend from the linear one (Non-  
235 Linearity parameter:  $NL$ ). A trend is defined as linear if the  $NL$  parameter is lower than 10%, indicating a small  
236 difference between ME and MK fits (Shatalov et al., 2015). In the following, the reported trends were analysed  
237 using the MK test for  $NL < 10\%$  and the ME test for  $NL > 10\%$ . More detailed description of the multi-exponential  
238 approach is available in the TFMM wiki and in the MSC-E Technical report 2015 (Shatalov et al., 2015).

239

## 240 3. Results

241 Results are presented and discussed in the following order: In Section 3.1, we compare the trends at both stations  
242 of  $PM_x$  concentrations from optical counters (OPC; annual data coverage around 90%) and from 24h gravimetric  
243 samples (filters; annual data coverage around 20-30%). This comparison will demonstrate the feasibility of  
244 studying trends of chemical species concentrations from filters despite the relatively low annual data coverage.  
245 In Section 3.2, we compare the magnitude of the trend of  $PM_{2.5}$  concentrations at MSY during 2004-2014 (period  
246 selected for this study) with the magnitude of trends calculated at the same station over different periods, namely  
247 2002-2010 (the period used in Cusack et al., 2012) and 2002-2014 (representing the largest period of gravimetric  
248  $PM_{2.5}$  measurements available at the time of writing at MSY station). This comparison was performed in order to  
249 study the differences in the trends over short periods (9 yr to 13 yr). The gravimetric concentrations of  $PM_{2.5}$   
250 measured at MSY were used with this aim. Then (Section 3.3), we present and discuss the trends at both stations  
251 of chemical species in both  $PM_{10}$  and  $PM_{2.5}$  from 24h filter analyses. In the Section 4.0 we discuss the sources of  
252 pollutants identified by PMF model in  $PM_{10}$  at both sites. Finally, we present and discuss the trends of  $PM_{10}$  source  
253 contributions at BCN and MSY (Section 4.1) providing possible explanations for the observed trends. Some  
254 conclusions are reported in Section 5.

255

### 256 3.1 Trends of PM: Comparison between gravimetric and real-time optical measurements

257 Annual data coverage is an important factor to take into account in order to study trends of a given parameter.  
258 The gravimetric PM measurements, from which chemical speciated data are obtained, are typically performed  
259 with rather low frequency over one year. In our case the annual data coverage of gravimetric measurements was  
260 around 20-30% at both Barcelona and Montseny. In this section we compare the trends of PM concentrations  
261 from gravimetric and real-time optical measurements (Table 1). Given that the trends of the considered  $PM_x$   
262 fractions were linear at both sites ( $NL < 10\%$ ), only results from MK test were reported in Table 1. However, we  
263 will show later (Section 4.1) that the contributions from specific  $PM_{10}$  pollutant sources from PMF model, mainly  
264 those related with anthropogenic activities, showed non-linear (i.e. exponential) decreasing trends, thus



265 mirroring the different effectiveness of the mitigation strategies depending on the source of pollutants  
266 considered.

267 As reported in Table 1, statistically significant decreasing trends were observed for the considered PM size  
268 fractions at BCN ( $-2.20 \mu\text{gm}^{-3}/\text{yr}$  with  $p<0.001$  for  $\text{PM}_{10}$  and  $-1.55 \mu\text{gm}^{-3}/\text{yr}$  with  $p<0.01$  for  $\text{PM}_{2.5}$  from OPC  
269 measurements), whereas at Montseny only the  $\text{PM}_{2.5}$  fraction showed a little significant decreasing trend ( $-0.26$   
270  $\mu\text{gm}^{-3}/\text{yr}$ ;  $p<0.1$  from OPC measurements). Total reductions (TR) ranged between 50.4% (OPC  $\text{PM}_{10}$  at BCN) to  
271 7.8% (OPC  $\text{PM}_{10}$  at MSY) and residual component (RC) was lower than 18% reflecting the goodness of the linear  
272 (MK) fit used. It must be noted that the higher p-values, magnitude of the trends and TR observed at BCN  
273 compared to MSY was likely due to the change of the measuring station in 2009 in BCN (cf. Fig. 1). Based on the  
274 comparison between simultaneous  $\text{PM}_x$  chemical speciated data collected at both BCN measurement sites during  
275 1 month (not shown) we concluded that after 2009 the BCN measuring site was less affected by mineral matter  
276 and, to a lesser extent, by road traffic emissions both being important sources of PM in Barcelona. In Figure 1 we  
277 highlighted the proximity of the BCN measuring station before 2009 to an unpaved parking and different  
278 construction works. The effect of the change of the station in BCN in 2009 on  $\text{PM}_{10}$  gravimetric measurements  
279 was reported in Supporting Information (Figure SI-1). However, despite the change of the station, the comparison  
280 between BCN and MSY for specific chemical species and pollutant sources not linked with mineral matter and  
281 road traffic emissions was possible.

282 Table 1 shows that the p-values calculated using gravimetric and OPC measurements was the same despite the  
283 different annual data coverage. The differences in the magnitude of the trends were 22% and 24% between  
284 gravimetric and OPC  $\text{PM}_{10}$  and  $\text{PM}_{2.5}$  measurements, respectively, at BCN and 24% and 21%, respectively, at MSY.  
285 Relative differences of total reductions (TR) ranged between 24% between gravimetric and OPC  $\text{PM}_{10}$   
286 measurements at MSY and 15% for  $\text{PM}_{10}$  at BCN. Thus, despite the different data coverage the magnitude of the  
287 trends and TR calculated from OPC and gravimetric measurements were rather similar. Other PM mass fractions  
288 ( $\text{PM}_{1-10}$  and  $\text{PM}_{2.5-10}$ ) and PM ratios ( $\text{PM}_1/\text{PM}_{10}$  and  $\text{PM}_{2.5}/\text{PM}_{10}$ ) at MSY showed non-statistically significant trends.

### 289 290 **3.2 Trends of PM: Comparison among different periods**

291 In this study we used the period 2004-2014 for trends analysis given that gravimetric  $\text{PM}_{2.5}$  measurements at BCN  
292 were available since 2004. Conversely, at MSY  $\text{PM}_{2.5}$  gravimetric measurements started in 2002. Figure 2 shows  
293 the trends of  $\text{PM}_{2.5}$  concentrations at MSY calculated using the MK test for the three different periods. ME test  
294 was not used here given that the observed trends were linear ( $\text{NL}<10\%$ ). The period 2002-2010 was the period  
295 considered in the paper from Cusack et al. (2012) presenting the trends of  $\text{PM}_{2.5}$  gravimetric mass and chemical  
296 species at MSY. The period 2002-2014 is the largest period with  $\text{PM}_{2.5}$  filter measurements available at the time  
297 of writing. The trend observed at MSY for the  $\text{PM}_{2.5}$  fraction during 2004-2014 confirmed what already observed  
298 by Cusack et al. (2012) at the same station for the period 2002 – 2010. In Cusack et al. (2012) the MK test provided

a decreasing trend of around  $-0.66 \mu\text{gm}^{-3}/\text{yr}$  at 0.01 significance level (TR = 35%). During the periods 2004 – 2014 and 2002 – 2014 decreasing trends of  $-0.33 \mu\text{gm}^{-3}/\text{yr}$  ( $p < 0.1$ ; TR = 26%) and  $-0.37 \mu\text{gm}^{-3}/\text{yr}$  ( $p < 0.05$ ; TR = 31%), respectively, were observed. Thus, a statistically significant trend for  $\text{PM}_{2.5}$  mass at regional level can be confirmed even considering different periods thus confirming the effectiveness of mitigation measures together with the effect of the economic crisis in Spain from 2008. However, it should be noted that the statistical significance of the trends observed for the larger periods was lower compared to Cusack et al. (2012). The difference observed in the magnitude of the trends during 2004-2014 compared to the results provided by Cusack et al. (2012) was mainly due to the increase of  $\text{PM}_{2.5}$  mass concentration in 2012 (cf. Figure 2). Chemical  $\text{PM}_{2.5}$  speciated data revealed that this increase was partly driven by organic matter showing a mean annual concentration in 2012 higher by around 20% compared to the 2004-2014 average.

309

### 3.3 Trends of chemical species

The trends of the annual mean concentrations of chemical species at BCN and MSY are reported in Table 2 (for  $\text{PM}_{10}$ ) and Table 3 (for  $\text{PM}_{2.5}$ ). Figure 3 (for BCN) and Figure 4 (for MSY) show the trends of chemical species in  $\text{PM}_{10}$ . In Tables 2 and 3 and Figures 3 and 4 only the species having statistically significant trends were reported.

As already noted, we assume that the change of the station in BCN in 2009 affected the trends of the concentrations of OC, EC, Cu, Sn, Sb and Zn (mainly traffic tracers),  $\text{Al}_2\text{O}_3$ , Ca, Mg, Ti, Rb, Sr (crustal elements related with both natural and anthropogenic sources) and Fe (traffic and crustal tracer). These chemical species at BCN were removed from Tables 2 and 3 and from Figure 3.

Other species with less local character measured in BCN were instead included in the analysis. These are  $\text{SO}_4^{2-}$ ,  $\text{NH}_4^+$ , V, Ni (related with heavy oil combustion in the study area according to source apportionment results, cf. Par. 4), Pb, Cd, and As (related with industrial/metallurgy activities), Na and Cl (sea spray), and  $\text{NO}_3^-$ . Although nitrate particles in Barcelona were mainly from traffic, the concentrations of these particles were not strongly affected by the change of the station due to their secondary origin. The MSY station will be considered as reference station given that no location change occurred at this monitoring site during the study period.

Statistically significant exponential trends ( $p < 0.01$  or 0.001) were mainly observed for the industrial tracers (Pb, Cd, As) in both  $\text{PM}_{10}$  and  $\text{PM}_{2.5}$ . For these elements TR was high and around 50-80% in  $\text{PM}_{10}$  and 67-81% in  $\text{PM}_{2.5}$ . The RCs were lower than 20% thus suggesting the goodness of the exponential fits used to study the trends of these species. Exponential fits were on average needed indicating that the trends were not gradual and consistent over time and that the effectiveness of the control measures for these pollutants was stronger at the beginning of the period under study (2004-2009 approximately) compared to the end of the period (Figs. 3 and 4). This is also evident by comparing the linear MK fit (dashed black line) with the ME fit (red line) in Figs. 3 and 4. In  $\text{PM}_{10}$  the magnitudes of the trends ranged between  $-0.00222 \mu\text{gm}^{-3}/\text{yr}$  (Pb;  $p < 0.001$ ) to  $-3.10\text{E-}5 \mu\text{gm}^{-3}/\text{yr}$  (Cd;  $p < 0.001$ ) at BCN and from  $-0.00031 \mu\text{gm}^{-3}/\text{yr}$  (Pb;  $p < 0.01$ ) to  $-1.12\text{E-}5 \mu\text{gm}^{-3}/\text{yr}$  (Cd;  $p < 0.01$ ) at MSY. In  $\text{PM}_{2.5}$  the

333 magnitude of the trends were similar and ranged between  $-0.00163 \mu\text{gm}^{-3}/\text{yr}$  (Pb;  $p<0.001$ ) and  $-3.11\text{E-}5 \mu\text{gm}^{-3}/\text{yr}$  (Cd;  $p<0.001$ ) at BCN and between  $-0.00049 \mu\text{gm}^{-3}/\text{yr}$  (Pb;  $p<0.001$ ) and  $-1.35\text{E-}5 \mu\text{gm}^{-3}/\text{yr}$  (Cd;  $p<0.001$ ) at MSY. Similar magnitude of the trends for these species in both PM fractions at both sites confirmed the common origin of these elements and the impact at regional scale of industrial sources. For Pb and Cd the characteristic time ( $\tau$ ) of the exponential trends was similar at both sites, whereas for As it was higher due to the slightly less intense exponential downward trend observed for As compared to Cd and Pb. Note that the PMF analysis (cf. Section 4) revealed that the concentrations of As were explained by multiple sources (especially at BCN) whereas the *Industrial/metallurgy* source alone explained more than around 70% of Pb and Cd concentrations (not shown). The implementation of the IPPC Directive in 2008 in Spain is the most probable cause for this downward trend. The decrease observed for Pb, Cd and As may be also attributed to a decrease in the emissions from industrial production (smelters, Querol et al., 2007) at a regional scale around Barcelona.

344 The concentrations of V and Ni in Barcelona in both  $\text{PM}_{10}$  and  $\text{PM}_{2.5}$  fractions showed very similar exponential decreasing trends. Similar characteristic times (around 10-11 yr), TR (around 59-63%) and RC (15-17%) in both fractions suggested the common and mainly fine origin of these two elements. At MSY, V and Ni showed linear trends likely because of the higher distance of the MSY station to the sources of V and Ni (shipping and, before 2008, energy production) compared to BCN. Note also that the NL parameter for BCN V and Ni was around 10-12%, indicating that in this case the exponential fit did not differ very much from the linear one. Total reduction for V and Ni at MSY was around 59-64% and 42-43%, respectively, and RCs were lower than 24%.

351 Sn and Cu in  $\text{PM}_{10}$  at MSY showed very similar behavior decreasing linearly with time with TR around 36-39% and RC around 16-20%. Decreasing rates of  $-3.65\text{E-}5 \mu\text{gm}^{-3}/\text{yr}$  ( $p<0.05$ ) and  $-0.00014 \mu\text{gm}^{-3}/\text{yr}$  ( $p<0.05$ ) were observed in  $\text{PM}_{10}$  for Sn and Cu, respectively. In  $\text{PM}_{2.5}$ , the concentrations of Sn and Cu decreased markedly compared to  $\text{PM}_{10}$  at the rate of  $-0.00084 \mu\text{gm}^{-3}/\text{yr}$  ( $p<0.001$ ) and  $-0.00026 \mu\text{gm}^{-3}/\text{yr}$  ( $p<0.01$ ), respectively. This difference could be explained by possible sources of coarser Sn and Cu which reduced the magnitude of the trends in  $\text{PM}_{10}$  mass fraction. Sb showed marked decreasing trends in both PM mass fractions compared to Sn and Cu with TR around 62-70%. The magnitude of the trends for Sb were similar in both fractions and around  $-3.57 \div -3.86\text{E-}5 \mu\text{gm}^{-3}/\text{yr}$ . Sb concentrations were better fitted with exponential curves (SE with  $p<0.01$  in  $\text{PM}_{10}$  and DE with  $p<0.01$  in  $\text{PM}_{2.5}$ ). The DE fit for Sb in  $\text{PM}_{2.5}$  had one positive and one negative characteristic time, the latter needed to explain the slight increase in Sb concentrations at the end of the considered period. The marked decreasing trend observed for Sb compared to other traffic tracers could be explained by a progressive reduction of Sb contained in the vehicle brakes. Cr did not show a statistically significant trend in both PM fractions.

363 Sulfate ( $\text{SO}_4^{2-}$ ) and ammonium ( $\text{NH}_4^+$ ) particles concentrations showed very similar behavior in  $\text{PM}_{2.5}$  and  $\text{PM}_{10}$  size fractions due to their fine nature. In BCN the magnitude of the trends were  $-0.37868 \mu\text{gm}^{-3}/\text{yr}$  ( $p<0.001$ ) and  $-0.11095 \mu\text{gm}^{-3}/\text{yr}$  ( $p<0.001$ ) for  $\text{SO}_4^{2-}$  and  $\text{NH}_4^+$ , respectively, in  $\text{PM}_{10}$  and  $-0.32778 \mu\text{gm}^{-3}/\text{yr}$  ( $p<0.001$ ) and  $-0.12701 \mu\text{gm}^{-3}/\text{yr}$  ( $p<0.001$ ), respectively, in  $\text{PM}_{2.5}$ . The trends were SE with very similar characteristic times (9.64-9.81 yr in  $\text{PM}_{10}$  and 9.69-10.53 yr in  $\text{PM}_{2.5}$ ), TR (64-65% in  $\text{PM}_{10}$  and 61-64% in  $\text{PM}_{2.5}$ ) and RC (12-14% in  $\text{PM}_{10}$  and

368 9-15% in PM<sub>2.5</sub>). At MSY the magnitude of the trends of SO<sub>4</sub><sup>2-</sup> and NH<sub>4</sub><sup>+</sup> and their statistical significance were  
369 lower compared to BCN in both fractions. Moreover, at MSY the trends were linear for SO<sub>4</sub><sup>2-</sup> in both fractions (as  
370 for V and Ni). These differences could be explained by the distance of MSY to direct specific sources of sulfate,  
371 such as shipping, compared to BCN, thus slightly reducing the magnitude and the statistical significance of the  
372 trend of SO<sub>4</sub><sup>2-</sup> at regional level. It is also interesting to note the similitude between the characteristic times of the  
373 exponential fits for V and Ni and SO<sub>4</sub><sup>2-</sup> in both PM fractions at BCN suggesting the main common origin of these  
374 chemical species. Possible reasons for the observed reduction in the concentrations of ambient sulfate in and  
375 around Barcelona will be discussed later.

376 Fine NO<sub>3</sub><sup>-</sup> (Table 3) showed statistically significant SE trends similar at both sites with p<0.001, TR around 73-82%,  
377 RC around 16-21% and characteristic times around 5.8-7.6 yr. In PM<sub>10</sub> the TR were lower and around 54-64% and  
378 the fits were linear at MSY and SE at BCN. The SE fit at BCN in PM<sub>10</sub> provided a characteristic time around 9.8 yr,  
379 higher compared to  $\tau$  obtained for the fine mode because fine NO<sub>3</sub><sup>-</sup> had a more pronounced downward trend  
380 compared to PM<sub>10</sub> NO<sub>3</sub><sup>-</sup>.

381 For the mineral species (Al<sub>2</sub>O<sub>3</sub>, Ca, Fe) linear (with the exception of Al<sub>2</sub>O<sub>3</sub> in PM<sub>2.5</sub> which was SE) and statistically  
382 significant decreasing trends were detected at MSY. On average the TR was higher in the fine fraction, ranging  
383 from 50% for Ca to 66% for Al<sub>2</sub>O<sub>3</sub>, compared to PM<sub>10</sub> (6-38% cf. Table 2). Downward decreasing trend for crustal  
384 material in PM<sub>2.5</sub> at MSY was also reported by Cusack et al. (2012) for the period 2002 – 2010 and by Querol et  
385 al. (2014) for the period 2001 – 2012. These trends were probably driven by weather conditions associated with  
386 negative NAO index (iNAO) that could be the cause for this slight reduction observed in crustal material. Pey et  
387 al. (2013) found a correlation between iNAO (calculated between June and September) and the contribution of  
388 Saharan dust to PM<sub>10</sub> mass in NE of Spain showing that the more negative is the iNAO the lower is the dust  
389 contribution to PM. The iNAO was unusually negative during the period 2008 – 2012  
390 (<http://www.cpc.ncep.noaa.gov/products/precip/CWlink/pna/norm.nao.monthly.b5001.current.ascii>) thus  
391 likely contributing to explain the observed trends of crustal elements. Moreover, negative NAO can favour the  
392 presence of fronts that can sweep the Iberian Peninsula from West to East causing higher wind and less stagnant  
393 conditions thus favouring the dispersion of pollutants. In addition, as suggested by Cusack et al (2012), it could  
394 also be hypothesised that some part of the crustal material measured at MSY is a product of the construction  
395 industry. The construction industry in Spain has been especially affected by the current economic recession, and  
396 crustal material produced by this industry may have contributed to the crustal load in PM<sub>2.5</sub>. For example, the  
397 number of home construction works in Barcelona during 2008 – 2014 (from the beginning of the economic crisis;  
398 mean number of works = 1281) reduced by around 75% compared to the period 2000 – 2007; mean number of  
399 works = 5187) (<http://www.bcn.cat/estadistica/castella/dades/timm/construccio/index.htm>). The fact that the  
400 total reduction calculated for mineral elements reported in Tables 2 and 3 was higher in PM<sub>2.5</sub> compared to PM<sub>10</sub>  
401 could corroborate this latter hypothesis.

402 Finally, Na concentrations showed linear decreasing trends at both sites, with the exception of PM<sub>10</sub> Na at MSY.  
403 Other species at MSY such as OC and EC did not show statistically significant trends. Consider that the  
404 concentrations of EC at MSY are very low and around at 0.2-0.3 µg/m<sup>3</sup> as annual mean. Both anthropogenic  
405 activity and biomass burning were expected to contribute to this chemical specie. Concerning OC the lack of trend  
406 was probably due to the contribution from biogenic sources to the concentration of this specie at regional level.

407

#### 408 4. PMF source profiles and contributions

409 Eight and seven sources were detected at BCN and MSY, respectively, in PM<sub>10</sub> from PMF model. The absolute and  
410 relative contributions of these sources to the measured PM<sub>10</sub> mass are reported in Figure 5. The chemical profiles  
411 of the detected sources were reported in Supporting Information (Figure SI-2).

412 Some of these sources were common at both BCN and MSY. These are: *Secondary Sulfate* (secondary inorganic  
413 source traced by SO<sub>4</sub><sup>2-</sup> and NH<sub>4</sub><sup>+</sup> and contributing 3.95 µg/m<sup>3</sup> (23.7%) and 4.67 µg/m<sup>3</sup> (13.7%) at MSY and BCN,  
414 respectively), *Secondary nitrate* (secondary inorganic source traced by NO<sub>3</sub><sup>-</sup> and NH<sub>4</sub><sup>+</sup> and contributing 1.31 µg/m<sup>3</sup>  
415 (7.9%) and 4.45 µg/m<sup>3</sup> (13.1%) at MSY and BCN, respectively), *V-Ni bearing* source (traced mainly by V, Ni and  
416 SO<sub>4</sub><sup>2-</sup> it represents the direct emissions from heavy oil combustion and contributed 0.71 µg/m<sup>3</sup> (4.3%) and 3.32  
417 µg/m<sup>3</sup> (9.8%) at MSY and BCN, respectively), *Mineral* (traced by typical crustal elements such as Al, Ca, Ti, Rb, Sr  
418 and contributing 2.70 µg/m<sup>3</sup> (16.2%) and 4.61 µg/m<sup>3</sup> (13.6%) at MSY and BCN, respectively), *Aged marine* (traced  
419 by Na and Cl mainly with contributions from SO<sub>4</sub><sup>2-</sup> and NO<sub>3</sub><sup>-</sup> and contributing 1.76 µg/m<sup>3</sup> (10.6%) and 5.73 µg/m<sup>3</sup>  
420 (16.9%) at MSY and BCN, respectively). Sources detected at MSY but not at BCN were: *Industrial/Traffic* source  
421 (traced by EC, OC, Cr, Cu, Zn, As, Cd, Sn, Sb and Pb it includes mixed contributions from anthropogenic sources  
422 such as road traffic and metallurgic industries and contributed 1.43 µg/m<sup>3</sup> (8.6%)) and *Aged organics* (traced  
423 mainly by OC and EC with maxima in summer indicating mainly a biogenic origin and contributing 3.78 µg/m<sup>3</sup>  
424 (22.7%)). The ratio OC:EC in the *Industrial/Traffic* and *Aged organic* source profiles at MSY were 4.2 and 11.7,  
425 respectively, thus indicating a strong influence of aged particles in the latter source with the former source being  
426 more fresh. The statistic of the OC:EC ratio based on chemical data at MSY is reported in Supporting Information  
427 (Figure SI-3). Mean and median values of OC:EC ratio at MSY were 9.1 and 7.8, respectively.

428 Finally, some sources were detected at BCN but not at MSY: *traffic* (traced by C<sub>nm</sub>, Cr, Cu, Sb and Fe mainly and  
429 contributing 5.14 µg/m<sup>3</sup> (15.1%)), *road/work resuspension* (traced by both crustal elements, mainly Ca, and traffic  
430 tracers such as Sb, Cu and Sn and contributing 4.25 µg/m<sup>3</sup> (12.5%)) and *Industrial/metallurgy* (traced by Pb, Cd,  
431 As and Zn and contributing 0.96 µg/m<sup>3</sup> (2.8%)).

432 A sensitivity study was performed in order to better interpret the PMF sources at BCN. In fact, for the period 2007  
433 – 2014 separate OC and EC concentration measurements were available and a PMF was performed. The  
434 comparison between the PMF source contributions obtained using the period 2007-2014 (separate OC and EC  
435 measurements) and the whole period (2004-2014; C<sub>nm</sub> (non-mineral carbon) available) is reported in Supporting

Information (Figure SI-4). As reported in Figure SI-4 the differences in source contribution and  $R^2$  ranged between -3% (*Mineral* source) and +20% (*Industrial* source) and 0.894 to 0.997, respectively, thus confirming the correct interpretation of the 2004-2014 PMF sources where  $C_{nm}$  was used. The OC:EC ratio in the *Traffic* source from 2007-2014 PMF was 1.70 (cf. Figure SI-5) whereas the mean and median OC:EC ratio from chemistry data were 2.5 and 2.3, respectively, thus being in agreement with the contribution of fresh particles from *Traffic* source at BCN.

442

#### 4.1 Trends of annual PM<sub>10</sub> source contributions

Figures 6 and 7 and Table 4 show the results from MK or ME test applied to the annual averages of PM<sub>10</sub> source contributions at BCN and MSY. As already noted we cannot study trends for *Traffic*, *Road/work resuspension* and *Mineral* source contributions at BCN because of the change of the station location in 2009. The contributions that showed statistically significant downward trends at both stations were from *Secondary sulfate*, *Secondary nitrate*, and *V-Ni bearing* sources ( $p < 0.001$  or  $p < 0.01$ ). Moreover, statistically significant decreasing trends were observed for the *Industrial/Traffic* ( $p < 0.01$ ) and *Mineral* ( $p < 0.1$ ) source contributions at MSY and the *Industrial/metallurgy* source ( $p < 0.001$ ) at BCN. These sources were mostly linked with anthropogenic activities and the observed decreasing trends confirmed the effectiveness of pollution control measures together with the possible effect of the economic crisis in Spain from 2008. Conversely, the contributions from sources mostly linked with natural processes such as *Aged Marine* (at both BCN and MSY) and *Aged Organic* (at MSY) did not show statistically significant trends.

The trends of the *Secondary sulfate* source contributions were DE and SE at BCN and MSY, respectively, thus the decrease over time of this source contribution was not gradual and monotonic. Overall the observed decreasing trends at both stations may be attributed to the legislation that came into force in 2007-2008 in Spain, the EC Directive on Large Combustion Plants, which resulted in the application of flue gas desulfurization (FGD) systems in a number of large facilities in 2007-2008 in Spain. Figure 8 shows the sharp decreases after 2007 observed for the national SO<sub>2</sub> and NO<sub>x</sub> emissions mostly from power generation (MAGRAMA, 2013; Querol et al., 2014). In BCN the two characteristic times (one low and the other high, cf. Table 4) of the DE fit indicated a strong decrease of the *Secondary sulfate* source contribution at the beginning of the period. Moreover, this decrease was sharper compared to MSY where SE fit was used. This difference was mostly due to the ban of heavy oils and petroleum coke for power generation around Barcelona from 2007. The effects of this AQ Regional Plan were likely more effective in BCN compared to MSY thus explaining the two different exponential fits used. Overall, for the *Secondary sulfate* source contributions the TRs were rather high around 53% at MSY and 67% at BCN with RC ranging from 16% (BCN) to 21% (MSY). The fact that the trend of the *Secondary sulfate* source contribution was exponential likely suggested the attainment of a lower limit and indicated a limited scope for further reduction of SO<sub>2</sub> emissions in our region. In fact, it has been estimated that the maximum in EU will be a further 20% reduction through measures in industry, residential and commercial heating and reduced agricultural waste

burning (UNECE, 2016). Conversely, in Eastern European countries the scope for reduction is much greater and around 60% (UNECE, 2016).

The trends of the *Secondary nitrate* source contributions were SE at both stations with very similar  $\tau$  (8.96 yr – 8.59 yr), TR (67-69 %) and RC (13-17%). The decrease observed for the contribution from the *Secondary Nitrate* source was related to the reduction in ambient  $\text{NO}_x$  concentrations (Figures 8 and 9). Figure 9 shows the levels of tropospheric  $\text{NO}_2$  column from 2005 to 2014 in South Europe from NASA  $\text{NO}_2$  OMI level3 plotted using the Giovanni online data system (Acker and Leptoukh, 2007). In Spain it can be observed a general decrease of the concentrations of columnar  $\text{NO}_2$  at regional level. Overall, the implementation of European directives affecting industrial and power generation emissions as well as the increase of the proportion of energy produced from renewable sources (cf. Figure 10 for Spain), among others, produced a significant reduction of  $\text{SO}_2$  and  $\text{NO}_x$  emissions. Around Barcelona the observed decreases were also attributed to the decrease of  $\text{NO}_x$  emissions mainly from the five power generation plants around the city. Moreover, the implementation during the 2008-2012 Regional AQ Plan of SCRT (continuously regenerating PM traps with selective catalytic reduction for  $\text{NO}_2$ ) and the hybridization and shift to natural gas engines of the Barcelona's bus fleet may have had an influence in the observed reductions.

The decreasing trends ( $p < 0.01$ ) of the *V-Ni bearing* source contributions were SE and L at BCN and MSY, respectively, reflecting the trends observed at both stations for the concentrations of V and Ni (cf. Table 2). At BCN the characteristic times ( $\tau$ ) was very similar to the characteristic times calculated for  $\text{PM}_{10}$  V and Ni (cf. Table 2) which were the main tracers of this source. TRs were around 61% at BCN and 64% at MSY and RCs were similar (19-25 %). The observed decrease in the *V-Ni bearing* source contribution was mainly attributed to the ban of the use of heavy oils and petroleum coke for power generation from 2008 in Spain.

The *Industrial/Metallurgy* source contribution at BCN decreased exponentially (SE) at the rate of  $-0.10 \mu\text{gm}^{-3}/\text{yr}$  ( $p < 0.001$ ) reflecting the SE decreasing trends observed for the main tracers of this pollutant source (Pb, Cd and As; cf. Table 2). The decrease of industrial emissions was mainly attributed to the implementation of IPPC (Integrated Pollution Prevention and Control) Directives. Moreover, the observed decrease may be attributed to a decrease in the emissions from industrial production (smelters, Querol et al., 2007) at a regional scale around Barcelona. Also, the financial crisis, whose impact on industrial production and use of fuels is evident since October 2008 also contributed to the observed trend. TR and RC for the *Industrial* source contributions at BCN were 65% and 16%, respectively. As for the contributions from *Secondary sulfate* and *nitrate* sources, the exponential trend observed for the *Industrial/Metallurgy* source contribution suggested the attainment of a lower limit. As evidenced in Fig. 6 the contribution from this source from 2010 was quite low and rather constant.

The contribution of the *Industrial/Traffic* source at MSY showed similar magnitude of the trend ( $-0.11 \mu\text{gm}^{-3}/\text{yr}$  with  $p < 0.01$ ) compared to the BCN *Industrial* contribution trend, being both sources traced mostly by the same industrial tracers. The trend of this source at MSY was linear with TR and RC of 56% and 13%, respectively, similar to those calculated for *Industrial* source contribution at BCN.

506 Finally, the *Mineral* source contribution at MSY showed linear little significant decreasing trend ( $p < 0.1$ ) in  
507 agreement with what observed at the same station by Cusack et al. (2012). As already noted in Section 3.3, this  
508 negative trend could be due to both a possible decrease of the emissions of finer anthropogenic mineral species  
509 from specific sources such as cement and concrete production and construction works and unusual weather  
510 conditions reducing Saharan dust contribution to PM and resuspension of dust.

511 In order to further interpret the observed trends, annual data on the annual National Energy Consumption (NECo)  
512 from different energy sources (MINETUR, 2013) were also evaluated (Figure 10). Overall, the primary energy  
513 consumption in Spain (NECo statistical data for Spain-MINETUR, 2013) increased from 2004 to 2007 and  
514 decreased from 2007 with marked decrease in 2009. Since 2009, the energy consumption indicator remained  
515 rather low and constant until 2012 when an additional decrease in 2013 and 2014 was observed. Oil consumption  
516 was fairly constant during 2004–2007 showing an important decrease during 2008–2014. This trend was probably  
517 governed by the fuel consumption for traffic road. Coal consumption remained constantly high from 2004 to 2007  
518 whereas, as for the emissions of  $\text{SO}_2$  (Fig. 8), a sharp decrease occurred from 2007. However, in the period 2011-  
519 2014 there was an important increase of coal consumption leading to an average consumption similar to the year  
520 2008. However, the implementation of FGD systems contributed to maintain  $\text{SO}_2$  at low concentrations, even in  
521 the coal production regions in Spain (cf. Querol et al., 2014). The hydroelectric generation was rather specular to  
522 coal consumption. For example, the increase in 2010 of hydroelectric consumption, due to high rainfall rate,  
523 mirrored the decrease in the coal consumption observed the same year. Finally, renewable energy consumption  
524 increased by 440% from 2004 to 2014, with a gradual growth in the NECo.

525

526

## 527 5.0 Conclusions

528 PM chemical speciated data collected at two twin stations in NE of Spain (Barcelona: urban background station  
529 and Montseny: regional background station) during 2004 – 2014 were used to study trends of source  
530 contributions from PMF analysis and of chemical species concentrations. Despite the fact the trends of different  
531 PM fractions ( $\text{PM}_{2.5}$  and  $\text{PM}_{10}$ ) were linear during the period under study, the trends of specific chemical elements  
532 and source contributions were exponential demonstrating the different effectiveness and time of implementation  
533 of different reduction strategies on specific pollutant sources. Statistically significant exponential trends ( $p < 0.01$   
534 or 0.001) were mainly observed for the industrial tracers (Pb, Cd, As) in both  $\text{PM}_{10}$  and  $\text{PM}_{2.5}$  and at both sites.  
535 The concentrations of V and Ni showed exponential trends in BCN and linear trends at MSY likely because of the  
536 higher distance of the MSY station to the sources of V and Ni (shipping and, before 2008, energy production)  
537 compared to BCN. Traffic tracers at MSY (Sn, Cu) showed very similar linear decreasing trends with higher  
538 magnitude of the trends in the fine ( $\text{PM}_{2.5}$ ) fractions compared to  $\text{PM}_{10}$  likely because of possible sources of  
539 coarser Sn and Cu reducing the magnitude of the trends in the  $\text{PM}_{10}$  mass fraction. Sb at MSY showed marked



540 exponential decreasing trends compared to other traffic tracers (Cu and Sn) which could be explained by a  
541 possible progressive reduction of Sb content in vehicle brakes. Secondary inorganic aerosols ( $\text{SO}_4^{2-}$ ,  $\text{NO}_3^-$  and  
542  $\text{NH}_4^+$ ) also showed marked decreasing trends (both linear and exponential) in both fractions and at both sites.  
543 However, in general the magnitude of the trends for these species and their statistical significance were higher  
544 at BCN compared to MSY.

545 The PM<sub>10</sub> source contributions that showed statistically significant downward trends at both Barcelona (BCN;  
546 UB) and Montseny (MSY; RB) were from *Secondary sulfate*, *Secondary nitrate*, and *V-Ni bearing* sources. For these  
547 source contributions the decreasing trends were exponential indicating that the trends were not gradual and  
548 consistent over time and that the effectiveness of the control measures for these pollutants was stronger at the  
549 beginning of the period under study (2004-2009 approximately) compared to the end of the period (Figs. 3 and  
550 4). Statistically significant decreasing trends were observed for the *Industrial/Traffic* and *Mineral* sources at MSY  
551 and the *Industrial/metallurgy* source at BCN. These sources were mostly linked with anthropogenic activities and  
552 the observed decreasing trends confirmed the effectiveness of pollution control measures implemented at EU or  
553 regional/local levels. The economic crisis which started in 2008 in Spain also contributed to the observed trends.  
554 Conversely, the contributions from sources mostly linked with natural processes such as *Aged Marine* (at both  
555 BCN and MSY) and *Aged Organic* (at MSY) did not show statistically significant trends. The general trends observed  
556 for the calculated PMF source contributions well reflected the trends observed for the chemical tracers of these  
557 pollutant sources. The decrease in the *Secondary sulfate* source contribution was mainly attributed to the EC  
558 Directive on Large Combustion Plants implemented from 2008 in Spain, resulting in the application of fuels gas  
559 desulfurization (FGD) systems in a number of large facilities. Moreover, according to the 2008 Regional AQ Plan,  
560 the use of heavy oils and petroleum coke for power generation was forbidden around Barcelona from 2008 in  
561 favour of natural gas. As a consequence, a decrease of the contributions from the V-Ni bearing source at both  
562 sites was also observed. The decrease observed for the contribution of the *Secondary Nitrate* source was mainly  
563 due to the reduction in ambient  $\text{NO}_x$  concentrations. In Spain a general decrease of the concentrations of  $\text{NO}_2$  at  
564 regional level was observed and it was mainly related with the lower energy consumption related with the  
565 financial crisis. The decrease of nitrates concentrations and *Secondary nitrate* source contributions around  
566 Barcelona was also attributed to the decrease of  $\text{NO}_x$  emissions from the five power generation plants around  
567 the city. Moreover, a Regional AQ Plan implementing the SCRT (continuously regenerating PM traps with selective  
568 catalytic reduction for  $\text{NO}_2$ ) and the hybridization and shift to natural gas engines of the Barcelona's bus fleet may  
569 have had also an influence in  $\text{NO}_x$  ambient concentrations. The *Industrial/Metallurgy* source contribution at BCN  
570 decreased exponentially reflecting the exponential trends observed for the main tracers of this pollutant source  
571 (Pb, Cd and As). The implementation of IPPC (Integrated Pollution Prevention and Control) Directives together  
572 with a decrease in the emissions from industrial production (smelters) at a regional scale around Barcelona  
573 explained the observed trends. Overall, the magnitude of the decreasing trends of the contributions of the  
574 pollutant sources were higher at BCN compared to MSY likely because of the proximity of the BCN measurement  
575 site to anthropogenic pollutant sources compared to the MSY site. The results presented in this work clearly

confirm the beneficial effect of the AQ measures taken in recent years in Europe. However, the WHO limit values of specific pollutants, PM<sub>10</sub> and PM<sub>2.5</sub> among these, are still exceeded especially at urban level and industrial hotspots. To meet the WHO guide levels important actions are still required for the next decade and the interpretation of past air quality trends may yield relevant outcomes for planning further cost-effective actions. We would like to highlight that a non-linear approach to trend studies is very attractive given that some air pollutants reported in this work showed not gradual-with-time reductions. Conversely, for specific pollutant source-contribution/concentration in our region, the decreasing trend was less steep at the end of the period compared to the beginning thus likely indicating the attainment of a lower limit. This was the case for example for the *Secondary sulfate* source contribution decreasing exponentially from 2004 to 2014 thus likely indicating a limited scope for further reduction of SO<sub>2</sub> emissions in our region.

586

## 587 **Acknowledgments.**

This work was supported by the MINECO (Spanish Ministry of Economy and Competitiveness), the MAGRAMA (Spanish Ministry of Agriculture, Food and Environment), the Generalitat de Catalunya (AGAUR 2014 SGR33 and the DGQA) and FEDER funds under the PRISMA project (CGL2012-39623- C02/00). The research leading to these results has received funding from the European Union's Horizon 2020 research and innovation programme under grant agreement No 654109 and previously from the European Union Seventh Framework Programme (FP7/2007-2013) under grant agreement n° 262254. Marco Pandolfi is funded by a Ramón y Cajal Fellowship (RYC-2013-14036) awarded by the Spanish Ministry of Economy and Competitiveness. NO<sub>2</sub> map analyses and visualizations used in this paper were produced with the Giovanni online data system, developed and maintained by the NASA GES DISC. The authors would like to express their gratitude to D. C. Carslaw and K. Ropkins for providing the Openair software used in this paper (Carslaw and Ropkins, 2012; Carslaw, 2012).

598

599

## 600 **Bibliography**

Acker, J. G. and Leptoukh, G.: *Online Analysis Enhances Use of NASA Earth Science Data*, Eos, Trans. AGU, 88, 2, 14-17, 2007.

Alastuey, A., Minguillón, M.C., Pérez, N., Querol, X., Viana, M. and de Leeuw, F.: *PM10 Measurement Methods and Correction Factors: 2009 Status Report*, ETC/ACM Technical Paper 2011/21, 2011.

Amato, F., M. Pandolfi, A. Escrig, X. Querol, A. Alastuey, J. Pey, N. Perez, P.K. Hopke, *Quantifying road dust resuspension in urban environment by Multilinear Engine: A comparison with PMF2*, Atmospheric Environment. 43 - 17, pp. 2770 - 2780. 06/2009, 2009.

608 Barmapadimos, I., Keller, J., Oderbolz, D., Hueglin, C., Prevot, A.S.H.: *One decade of parallel fine (PM<sub>2.5</sub>) and coarse*  
609 *(PM<sub>10</sub>–PM<sub>2.5</sub>) particulate matter measurements in Europe: trends and variability*, Atmos Chem Phys, 12, 3189–  
610 3203, <http://dx.doi.org/10.5194/acp-12-3189-2012>, 2012

611 Carslaw, D.C., *The OpenAir manual — open-source tools for analysing air pollution data*, Manual for version 0.5-  
612 16, King's College, London, 2012.

613 Carslaw, D.C., Ropkins, K.: *OpenAir — an R package for air quality data analysis*, Environ Model Softw, 27–28, 52–  
614 61, 2012

615 Cavalli, F., Viana, M., Yttri, K. E., Genberg, J., and Putaud, J.-P.: *Toward a standardised thermal-optical protocol*  
616 *for measuring atmospheric organic and elemental carbon: the EUSAAR protocol*, Atmos. Meas. Tech., 3, 79-89,  
617 doi:10.5194/amt-3-79-2010, 2010.

618 Cusack, M., Alastuey, A., Perez, N., Pey, J., Querol, X.: *Trends of particulate matter (PM<sub>2.5</sub>) and chemical*  
619 *composition at a regional background site in the Western Mediterranean over the last nine years (2002–2010)*,  
620 Atmos Chem Phys, 12, 8341–8357 <http://dx.doi.org/10.5194/acp-12-8341-2012>, 2012.

621 EEA: European Environmental Agency Air quality in Europe — 2013 report, EEA report 9/2013, Copenhagen, 1725-  
622 9177, [107 pp. <http://www.eea.europa.eu/publications/air-quality-in-europe-2013>], 2013.

623 EEA: European Environmental Agency Air quality in Europe — 2015 report, *Many Europeans still exposed to*  
624 *harmful air pollution. Air pollution is the single largest environmental health risk in Europe*, EEA report 11/2015,  
625 Copenhagen, 1-7, [[http://www.eea.europa.eu/media/newsreleases/many-europeans-still-exposed-to-air-](http://www.eea.europa.eu/media/newsreleases/many-europeans-still-exposed-to-air-pollution-2015)  
626 [pollution-2015](http://www.eea.europa.eu/media/newsreleases/many-europeans-still-exposed-to-air-pollution-2015)], 2015.

627 Escrig, A., Monfort, E., Celades, I., Querol, X., Amato, F., Min guillon, M. C., and Hopke, P. K.: *Application of*  
628 *optimally scaled target factor analysis for assessing source contribution of ambi ent PM<sub>10</sub>*, J. Air Waste Manage.,  
629 59(11), 1296–1307, 2009.

630 Gilbert, R.O.: *Statistical Methods for Environmental Pollution Monitoring*, Wiley, NY, 1987.

631 Guerreiro, C., Leeuw, F. de, Foltescu, V., Horálek, J., & European Environment Agency: *Air quality in Europe 2014*  
632 *report*, Luxembourg: Publications Office.  
633 <http://bookshop.europa.eu/uri?target=EUB:NOTICE:THAL14005:EN:HTML>, 2014

634 Harrison, R.M., Stedman, J., Derwent, D.: *New directions: why are PM<sub>10</sub> concentrations in Europe not falling?*,  
635 Atmos Environ, 42, 603–606, 2008.

636 Henschel, S., Querol, X., Atkinson, R., Pandolfi, M., Zeca, A., Le Tertre, A., Analitis, A., Katsouyanni, K., Chanel, O.,  
637 Pascal, M., Bouland, C., Haluza, D., Medina, S., Goodman, P.G.: *Ambient air SO<sub>2</sub> patterns in 6 European cities*,  
638 Atm. Env., 79, 236 - 247. 11/2013, 2013.

639 Henschel, S., Le Tertre, A., Atkinson, R.W., Querol, X., Pandolfi, M., Zeka, A., Haluza, D., Antonis, A., Katsouyanni,  
640 K., Bouland, C., Pascal, M., Medina, S., Goodman, P.G.: *Trends of nitrogen oxides in ambient air in nine European*  
641 *cities between 1999 and 2010*, *Atm. Env.* 117, 234 - 241. 09/2015, 2015.

642 Kendall, M.G.: *Rank Correlation Methods*, 4th edition, Charles Griffin, London, 1975.

643 MAGRAMA. Inventario Nacional de Emisiones de Contaminantes a la Atmósfera. Ministerio de Agricultura,  
644 Alimentación y Medio Ambiente del Gobierno de España. [http://www.magrama.gob.es/ca/calidad-y-evaluacion-](http://www.magrama.gob.es/ca/calidad-y-evaluacion-ambiental/temas/sistemaespanol-de-inventario-sei-/)  
645 [ambiental/temas/sistemaespanol-de-inventario-sei-/](http://www.magrama.gob.es/ca/calidad-y-evaluacion-ambiental/temas/sistemaespanol-de-inventario-sei-/), 2013.

646 Mann, H.B.: *Non-parametric tests against trend*, *Econometrica* 13:163-171, 1945.

647 MINETUR. Ministerio de Industria, Energía y Turismo. Gobierno de España: energy statistics and balances.  
648 <http://www.minetur.gob.es/energia/balances/Balances/Paginas/CoyunturaTrimestral.aspx>, 2013.

649 Paatero, P. and Tapper, U.: *Positive Matrix Factorization: a non negative factor model with optimal utilization of*  
650 *error estimates of data values*, *Environmetrics*, 5, 111–126, 1994.

651 Paatero, P.: *Least squares formulation of robust non-negative factor analysis*, *Chemometr. Intell. Lab.*, 37, 23–35,  
652 1997.

653 Paatero, P., Hopke, P. K., Song, X., and Ramadan, Z.: *Understanding and controlling rotations in factor analytic*  
654 *models*, *Chemometrics and Intelligent Laboratory Systems*, 60(1–2), 253–264, 2002.

655 Paatero, P. and Hopke, P. K.: *Discarding or downweighting high noise variables in factor analytic models*, *Anal.*  
656 *Chim. Acta*, 490, 277–289, doi:10.1016/s0003-2670(02)01643-4, 2003.

657 Paatero P.: User's guide for positive matrix factorization programs PMF2 and PMF3, Part1: tutorial. University of  
658 Helsinki, Helsinki, Finland, 2004.

659

660 Paatero, P., Hopke, P. K., Begum, B. A., and Biswas, S. K.: *A graphical diagnostic method for assessing the rotation*  
661 *in factor analytical models of atmospheric pollution*, *Atmos. Environ.*, 39, 193–201,  
662 doi:10.1016/j.atmosenv.2004.08.018, 2005.

663 Pandolfi, M., Cusack, M., Alastuey, a. and Querol, X.: *Variability of aerosol optical properties in the Western*  
664 *Mediterranean Basin*, *Atmos. Chem. Phys.*, 11(15), 8189–8203, doi:10.5194/acp-11-8189-2011, 2011.

665 Pandolfi, M., F. Amato, C. Reche, A. Alastuey, R. P. Otjes, M. J. Blom, X. Querol, *Summer ammonia measurements*  
666 *in a densely populated Mediterranean city*, *Atmospheric Chemistry and Physics*. 12, pp. 7557 - 7575. 08/2012,  
667 2012.

668 Pandolfi, M., G. Martucci, X. Querol, A. Alastuey, F. Wilsenack, S. Frey, C.D. O'Dowd, M. Dall'Osto, *Continuous*  
669 *atmospheric boundary layer observations in the coastal urban area of Barcelona during SAPUSS*, Atmospheric  
670 Chemistry and Physics. 13 - 9, pp. 4983 - 4996. 05/2013, 2013.

671 Pandolfi, M., Querol, X., Alastuey, A., Jimenez, J. L., Jorba, O., Day, D., Ortega, A., Cubison, M. J., Comerón, A.,  
672 Sicard, M., Mohr, C., Prévôt, A. S. H., Minguillón, M. C., Pey, J., Baldasano, J. M., Burkhardt, J. F., Seco, R., Peñuelas,  
673 J., van Drooge, B. L., Artiñano, B., Di Marco, C., Nemitz, E., Schallhart, S., Metzger, A., Hansel, A., Lorente, J., Ng,  
674 S., Jayne, J. and Szidat, S.: Effects of sources and meteorology on particulate matter in the Western Mediterranean  
675 Basin: An overview of the DAURE campaign, J. Geophys. Res. Atmos., 119(8), 4978–5010,  
676 doi:10.1002/2013JD021079, 2014.

677 Pérez, N., Pey, J., Castillo, S., Viana, M., Alastuey, A. and Querol, X.: Interpretation of the variability of levels of  
678 regional background aerosols in the Western Mediterranean, Sci. Total Environ., 407(1), 527–540,  
679 doi:10.1016/j.scitotenv.2008.09.006, 2008.

680 Pey, J., Pérez, N., Querol, X., Alastuey, A., Cusack, M. and Reche, C.: Intense winter atmospheric pollution episodes  
681 affecting the Western Mediterranean., Sci. Total Environ., 408(8), 1951–9, doi:10.1016/j.scitotenv.2010.01.052,  
682 2010.

683 Pey, J., Querol, X., Alastuey, A., Forastiere, F., and Stafoggia, M.: African dust outbreaks over the Mediterranean  
684 Basin during 2001–2011: PM10 concentrations, phenomenology and trends, and its relation with synoptic and  
685 mesoscale meteorology, Atmos. Chem. Phys., 13, 1395-1410, doi:10.5194/acp-13-1395-2013, 2013.

686 Querol, X., Viana, M., Alastuey, A., Amato, F., Moreno, T., Castillo, S., Pey, J., de la Rosa, J., Artiñano, B., Salvador,  
687 P., García Dos Santos, S., Fernández-Patier, R., Moreno-Grau, S., Negral, L., Minguillón, M.C., Monfort, E., Gil, J.I.,  
688 Inza, A., Ortega, L.A., Santamaría, J.M., Zabalza, J.: Source origin of trace elements in PM from regional  
689 background, urban and industrial sites of Spain, Atm. Env., 41, 7219-7231, 2007.

690 Querol, X., Alastuey, A., Moreno, T., Viana, M.M., Castillo, S., Pey, J., Rodríguez, S., Artiñano, B., Salvador, P.,  
691 Sánchez, M., García Dos Santos, S., Herce Garraleta, M.D., Fernandez-Patier, R., Moreno-Grau, S., Negral, L.,  
692 Minguillón, M.C., Monfort, E., Sanz, M.J., Palomo-Marín, R., Pinilla-Gil, E., Cuevas, E., de la Rosa, J., Sánchez de la  
693 Campa, A.: *Spatial and temporal variations in airborne particulate matter (PM10 and PM2.5) across Spain 1999–*  
694 *2005*, Atm. Env., 42, 3694–3979, 2008.

695 Querol, X., M. Viana, T. Moreno, A. Alastuey, J. Pey, F. Amato, M. Pandolfi, et al., *Scientific bases for a National*  
696 *Air Quality Plan* (in Spanish), Colección Informes CSIC, 978-84-00-09475-1, 3, 2012.

697 Querol, X., , Alastuey, A., Pandolfi, M., Reche, C., Pérez, N., Minguillón, M.C., Moreno, T., Viana, M., Escudero, M.,  
698 Orio, A., Pallarés, M., Reina, F.: *2001–2012 trends on air quality in Spain*, Science of The Total Environment, 490,  
699 957–969, doi:10.1016/j.scitotenv.2014.05.074, 2014

700 Salmi, T., Maata, A., Antilla, P., Ruoho-Airola, T., Amnell, T.: Detecting trends of annual values of atmospheric  
701 pollutants by the Mann Kendall test and Sen's slope estimates – the Excel template application Makesens, Finnish  
702 Meteorological Institute, Helsinki, Finland, 35 pp, 2002.

703 Salvador P., Artiñano B., Viana M., Alastuey A., Querol X.: *Evaluation of the changes in the Madrid metropolitan*  
704 *area influencing air quality: analysis of 1999-2008 temporal trend of Particulate Matter*, Atmos. Environ., 57, 175-  
705 185, 2012.

706

707 Sen, P.K., *Estimates of regression coefficient based on Kendall's tau*, J Am Stat Assoc, 63, 1379–1389, 1968

708 Shatalov V., Ilyin I., Gusev A., Rozovskaya O., Travnikov O.: *Heavy Metals and Persistent Organic Pollutants:*  
709 *development of multi-scale modeling and trend analysis methodology*. EMEP/MSC-E Technical report 1/2015,  
710 2015.

711 Smith, D.M.: *Computing single parameter transformations*, Communications in Statistics - Simulation and  
712 Computation, 32, 605-618, 2002.

713 Theil, H.: *A rank invariant method of linear and polynomial regression analysis, I, II, III*, Proceedings of the  
714 Koninklijke Nederlandse Akademie Wetenschappen, SeriesA — Mathematical Sciences, 386–392, 521–525,  
715 1397–1412, 1950.

716 UNECE: Towards Cleaner Air. Scientific Assessment Report. EMEP Steering Body and Working Group on Effects of  
717 the Convention on Long-Range Transboundary Air Pollution, Oslo. xx+50pp, Eds. Maas, R., P. Grennfelt,  
718 [www.unece.org/environmental-policy/conventions/envlirtapwelcome/publications.html](http://www.unece.org/environmental-policy/conventions/envlirtapwelcome/publications.html), 2016.

719 Williams, M.L., D. Carslaw, *New directions: science and policy — out of step on NOx and NO2?* Atmos Environ, 45,  
720 3911–3912, 2011.

721

722

723

724

725

726

727

728

729 **Table 1:** Trends of different PM mass fractions from gravimetry (grav) and optical (OPC) measurements at BCN (bold italic) and MSY (2004-  
730 2014). TR (%) = Total Reduction; RC (%) = Residual Component. Significance of the trends following the Mann-Kendall test: \*\*\* (p-value <  
731 0.001), \*\* (p-value < 0.01), \* (p-value < 0.05), + (p-value < 0.1).

PM <sub>x</sub>	PM <sub>x</sub>		Mann-Kendall fit			
Fraction	Conc. 2004 (µgm <sup>-3</sup> )	Conc. 2014 (µgm <sup>-3</sup> )	p- value	Trend [µgm <sup>-3</sup> /yr]	TR [%]	RC [%]
PM <sub>10</sub> (grav.)	<b><i>41.1</i></b>	<b><i>19.2</i></b>	***	<b><i>-2.83</i></b>	<b><i>59.2</i></b>	<b><i>8.5</i></b>
	19.2	13.9		-0.17	10.5	17.6
PM <sub>2.5</sub> (grav.)	<b><i>31.6</i></b>	<b><i>13.2</i></b>	***	<b><i>-2.03</i></b>	<b><i>60.1</i></b>	<b><i>7.9</i></b>
	16.2	9.8	+	-0.33	25.6	17.3
PM <sub>10</sub> (OPC)	<b><i>39.1</i></b>	<b><i>19.8</i></b>	***	<b><i>-2.20</i></b>	<b><i>50.4</i></b>	<b><i>10.0</i></b>
	18.6	12.3		-0.13	7.8	16.9
PM <sub>2.5</sub> (OPC)	<b><i>27.1</i></b>	<b><i>12.9</i></b>	**	<b><i>-1.55</i></b>	<b><i>49.6</i></b>	<b><i>9.8</i></b>
	16.5	9.3	+	-0.26	21.2	17.5

**Table 2:** Mann-Kendall and Multi-exponential trends of different chemical species in PM<sub>10</sub> at BCN (bold italic) and MSY. Type of trend: linear (L), single-exponential (SE), double exponential (DE); **a** (μgm<sup>-3</sup>) and **τ** (yr) are the constants and the characteristic times, respectively, of the exponential data fittings; NL (%) = Non-Linearity; TR (%) = Total Reduction; RC (%) = Residual Component; ns = not statistically significant; ni = not included. Significance of the trends: \*\*\* (p-value < 0.001), \*\* (p-value < 0.01), \* (p-value < 0.05), + (p-value < 0.1).

Specie	PM <sub>10</sub> (BCN:MSY)		Fit type	NL (%)	p- value	Mann- Kendall fit Trend [μgm <sup>-3</sup> /yr]	Multi-exponential fit			TR (%)	RC (%)
	Concentration 2004 (μgm <sup>-3</sup> )	Concentration 2014 (μgm <sup>-3</sup> )					a (μgm <sup>-3</sup> )	τ (yr)	Trend [μgm <sup>-3</sup> /yr]		
Pb	<b><i>0.02685</i></b>	<b><i>0.00694</i></b>	<b><i>SE</i></b>	<b>27</b>	***		<b><i>0.03246</i></b>	<b><i>6.12</i></b>	<b><i>-0.00222</i></b>	<b>80</b>	<b>17</b>
	0.00481	0.00190	SE	11	**		0.00553	10.22	-0.00031	62	13
Cd	<b><i>0.00043</i></b>	<b><i>0.00015</i></b>	<b><i>SE</i></b>	<b>19</b>	***		<b><i>0.00048</i></b>	<b><i>7.59</i></b>	<b><i>-3.10e-5</i></b>	<b>73</b>	<b>17</b>
	0.00017	0.00006	SE	18	**		0.00018	7.92	-1.12E-5	72	16
As	<b><i>0.00094</i></b>	<b><i>0.00036</i></b>	<b><i>SE</i></b>	<b>14</b>	***		<b><i>0.00118</i></b>	<b><i>9.11</i></b>	<b><i>-7.07E-5</i></b>	<b>67</b>	<b>11</b>
	0.00029	0.00017	L	<10	***	-1.29E-5				50	9
V	<b><i>0.01116</i></b>	<b><i>0.00454</i></b>	<b><i>SE</i></b>	<b>12</b>	**		<b><i>0.01502</i></b>	<b><i>10.04</i></b>	<b><i>-0.00086</i></b>	<b>63</b>	<b>17</b>
	0.00328	0.00175	L	<10	**	-0.00022				59	15
Ni	<b><i>0.00531</i></b>	<b><i>0.00284</i></b>	<b><i>SE</i></b>	<b>11</b>	***		<b><i>0.00678</i></b>	<b><i>10.61</i></b>	<b><i>-0.00037</i></b>	<b>61</b>	<b>16</b>
	0.00155	0.00100	L	<10	**	-7.10E-5				43	20
Sn	<b><i>ni</i></b>	<b><i>ni</i></b>									
	0.00127	0.00057	L	<10	*	-3.65E-5				39	16
Cu	<b><i>ni</i></b>	<b><i>ni</i></b>									
	0.00420	0.00216	L	<10	*	-0.00014				36	20
Sb	<b><i>ni</i></b>	<b><i>ni</i></b>									
	0.00058	0.00025	SE	11	**		0.00064	10.46	-3.57E-5	62	13
SO <sub>4</sub> <sup>2-</sup>	<b><i>5.74436</i></b>	<b><i>2.28596</i></b>	<b><i>SE</i></b>	<b>12</b>	***		<b><i>6.56033</i></b>	<b><i>9.81</i></b>	<b><i>-0.37868</i></b>	<b>64</b>	<b>12</b>
	2.84849	1.67712	L	<10	**	-0.11836				42	18
NO <sub>3</sub> <sup>-</sup>	<b><i>5.07816</i></b>	<b><i>1.72401</i></b>	<b><i>SE</i></b>	<b>12</b>	**		<b><i>6.49890</i></b>	<b><i>9.83</i></b>	<b><i>-0.37484</i></b>	<b>64</b>	<b>15</b>
	1.80724	0.67419	L	<10	**	-0.10593				54	13
NH <sub>4</sub> <sup>+</sup>	<b><i>1.92062</i></b>	<b><i>0.57008</i></b>	<b><i>SE</i></b>	<b>12</b>	***		<b><i>1.90645</i></b>	<b><i>9.64</i></b>	<b><i>-0.11095</i></b>	<b>65</b>	<b>14</b>
	1.14268	0.40135	SE	13	*		1.28868	9.26	-0.07640	66	22
Al <sub>2</sub> O <sub>3</sub>	<b><i>ni</i></b>	<b><i>ni</i></b>									
	0.72357	0.46382	L	<10	*	-0.02383				34	18
Ca	<b><i>ni</i></b>	<b><i>ni</i></b>									
	0.42703	0.28279	L	<10	*	-0.01638				38	17
Fe	<b><i>ni</i></b>	<b><i>ni</i></b>									
	0.22371	0.14895	L	<10	+	-0.00593				6	44
Na	<b><i>1.02188</i></b>	<b><i>0.77408</i></b>	<b><i>L</i></b>	<b>&lt;10</b>	*	<b><i>-0.03943</i></b>				<b>34</b>	<b>12</b>
					ns						



765

766

767

768

769

770

771

772

773

774

775

776

777

778

**Table 3:** Mann-Kendall and Multi-exponential trends of different chemical species in PM<sub>2.5</sub> at BCN (bold italic) and MSY. Type of trend: linear (L), single-exponential (SE), double exponential (DE); **a** (μgm<sup>-3</sup>) and **τ** (yr) are the constants and the characteristic times, respectively, of the exponential data fittings; NL (%) = Non-Linearity; TR (%) = Total Reduction; RC (%) = Residual Component; ns = not statistically significant; ni = not included. Significance of the trends: \*\*\* (p-value < 0.001), \*\* (p-value < 0.01), \* (p-value < 0.05), + (p-value < 0.1).

Specie	PM <sub>2.5</sub> (BCN;MSY)		Fit type	NL (%)	p-value	Mann-Kendall fit	Multi-exponential fit			TR (%)	RC (%)
	Concentration 2004 (μgm <sup>-3</sup> )	Concentration 2014 (μgm <sup>-3</sup> )				Trend [μgm <sup>-3</sup> /yr]	a (μgm <sup>-3</sup> )	τ (yr)	Trend [μgm <sup>-3</sup> /yr]		
Pb	<b><i>0.02117</i></b>	<b><i>0.00500</i></b>	<b><i>SE</i></b>	<b><i>27</i></b>	<b><i>***</i></b>		<b><i>0.02390</i></b>	<b><i>6.24</i></b>	<b><i>-0.00163</i></b>	<b><i>80</i></b>	<b><i>13</i></b>
	0.00642	0.00149	SE	28	***		0.00716	6.08	-0.00049	81	18
Cd	<b><i>0.00041</i></b>	<b><i>0.00011</i></b>	<b><i>SE</i></b>	<b><i>23</i></b>	<b><i>***</i></b>		<b><i>0.00047</i></b>	<b><i>6.81</i></b>	<b><i>-3.11E-5</i></b>	<b><i>77</i></b>	<b><i>13</i></b>
	0.00020	0.00005	SE	23	***		0.00020	6.77	-1.35E-5	77	18
As	<b><i>0.00069</i></b>	<b><i>0.00027</i></b>	<b><i>SE</i></b>	<b><i>14</i></b>	<b><i>***</i></b>		<b><i>0.00091</i></b>	<b><i>9.00</i></b>	<b><i>-5.43E-5</i></b>	<b><i>67</i></b>	<b><i>11</i></b>
	0.00029	0.00013	SE	15	**		0.00033	8.56	-2.04E-5	69	19
V	<b><i>0.00823</i></b>	<b><i>0.00368</i></b>	<b><i>SE</i></b>	<b><i>11</i></b>	<b><i>**</i></b>		<b><i>0.01121</i></b>	<b><i>11.13</i></b>	<b><i>-0.00061</i></b>	<b><i>59</i></b>	<b><i>16</i></b>
	0.00271	0.00130	L	<10	**	-0.00017				64	24
Ni	<b><i>0.00402</i></b>	<b><i>0.00185</i></b>	<b><i>SE</i></b>	<b><i>10</i></b>	<b><i>**</i></b>		<b><i>0.00498</i></b>	<b><i>11.23</i></b>	<b><i>-0.00027</i></b>	<b><i>59</i></b>	<b><i>15</i></b>
	0.00189	0.00080	SE	13	**		0.00205	9.36	-0.00012	42	21
Sn	<b><i>ni</i></b>	<b><i>ni</i></b>									
	0.00157	0.00043	L	<10	***	-0.00084				61	12
Cu	<b><i>ni</i></b>	<b><i>ni</i></b>									
	0.00394	0.00113	SE	14	**		0.00426	8.99	-0.00026	67	13
Sb	<b><i>ni</i></b>	<b><i>ni</i></b>									
	0.00053	0.00015	DE	48	**		0.00069 1.3E-6	4.52 -2.50	-3.86E-5	70	16
SO <sub>4</sub> <sup>2-</sup>	<b><i>4.86564</i></b>	<b><i>1.92388</i></b>	<b><i>SE</i></b>	<b><i>12</i></b>	<b><i>***</i></b>		<b><i>5.64582</i></b>	<b><i>9.69</i></b>	<b><i>-0.32778</i></b>	<b><i>64</i></b>	<b><i>9</i></b>
	2.98922	1.43381	L	<10	**	-0.16222				54	15
NO <sub>3</sub> <sup>-</sup>	<b><i>3.45513</i></b>	<b><i>0.86002</i></b>	<b><i>SE</i></b>	<b><i>19</i></b>	<b><i>***</i></b>		<b><i>4.14459</i></b>	<b><i>7.61</i></b>	<b><i>-0.26753</i></b>	<b><i>73</i></b>	<b><i>16</i></b>
	1.66095	0.29452	SE	30	***		1.96014	5.81	-0.13550	82	21
NH <sub>4</sub> <sup>+</sup>	<b><i>2.19735</i></b>	<b><i>0.68393</i></b>	<b><i>SE</i></b>	<b><i>11</i></b>	<b><i>***</i></b>		<b><i>2.27813</i></b>	<b><i>10.53</i></b>	<b><i>-0.12701</i></b>	<b><i>61</i></b>	<b><i>15</i></b>
	1.39366	0.48049	SE	18	**		1.62588	7.94	-0.10266	72	14
Al <sub>2</sub> O <sub>3</sub>	<b><i>ni</i></b>	<b><i>ni</i></b>									
	0.30245	0.10153	SE	13	*		0.26678	9.36	-0.01574	66	35
Ca	<b><i>ni</i></b>	<b><i>ni</i></b>									
	0.11478	0.06540	L	<10	+	-0.00494				50	33
Fe	<b><i>ni</i></b>	<b><i>ni</i></b>									
	0.09679	0.03716	L	<10	*	-0.00504				61	31
Na	<b><i>0.27476</i></b>	<b><i>0.17863</i></b>	<b><i>L</i></b>	<b><i>&lt;10</i></b>	<b><i>+</i></b>	<b><i>-0.01247</i></b>				<b><i>41</i></b>	<b><i>15</i></b>
	0.13091	0.07252	L	<10	*	-0.00584				45	18

779

780

781

782

783

784

785

786

787

788

789

790

791

792

793

794

795

796

797

798

799

**Table 4:** Mann-Kendall and Multi-exponential trends of source contributions in PM<sub>10</sub> from PMF at BCN (bold italic) and MSY. Type: linear (L), single-exponential (SE), double exponential (DE); **a** (μgm<sup>-3</sup>) and **τ** (yr) are the constants and the characteristic times, respectively, of the exponential data fittings; NL (%) = Non-Linearity; TR (%) = Total Reduction; RC (%) = Residual Component; ni = not included . Significance of the trends following the Mann-Kendall test: \*\*\* (p-value < 0.001), \*\* (p-value < 0.01), \* (p-value < 0.05), + (p-value < 0.1).

Source	PM <sub>10</sub> (BCN:MSY)		Fit type	NL (%)	p-value	Mann- Kendall fit	Multi-exponential fit			TR (%)	RC (%)
	Contribution 2004 (μgm <sup>-3</sup> )	Contribution 2014 (μgm <sup>-3</sup> )				Trend [μgm <sup>-3</sup> /yr]	a (μgm <sup>-3</sup> )	τ (yr)	Trend [μgm <sup>-3</sup> /yr]		
<i>Secondary sulfate</i>	<b><i>10.27</i></b>	<b><i>3.38</i></b>	<b><i>DE</i></b>	<b><i>45</i></b>	<b><i>**</i></b>		<b><i>12.33</i></b> <b><i>3.82</i></b>	<b><i>1.65</i></b> <b><i>105.80</i></b>	<b><i>-0.71</i></b>	<b><i>67</i></b>	<b><i>16</i></b>
	6.57	3.07	SE	12	**		5.99	13.22	-0.32	53	21
<i>Secondary nitrate</i>	<b><i>6.99</i></b>	<b><i>1.96</i></b>	<b><i>SE</i></b>	<b><i>14</i></b>	<b><i>***</i></b>		<b><i>8.54</i></b>	<b><i>8.96</i></b>	<b><i>-0.51</i></b>	<b><i>67</i></b>	<b><i>13</i></b>
	2.03	0.47	SE	15	**		2.44	8.59	-0.15	69	17
<i>V-Ni bearing</i>	<b><i>4.23</i></b>	<b><i>1.84</i></b>	<b><i>SE</i></b>	<b><i>11</i></b>	<b><i>**</i></b>		<b><i>5.66</i></b>	<b><i>10.59</i></b>	<b><i>-0.32</i></b>	<b><i>61</i></b>	<b><i>19</i></b>
	0.79	0.44	L	8	**	-0.07				64	25
<i>Industrial/Metallurgy (BCN)</i>	<b><i>1.64</i></b>	<b><i>0.71</i></b>	<b><i>SE</i></b>	<b><i>21</i></b>	<b><i>***</i></b>		<b><i>1.76</i></b>	<b><i>9.56</i></b>	<b><i>-0.10</i></b>	<b><i>65</i></b>	<b><i>16</i></b>
<i>Mineral</i>	<b><i>ni</i></b>	<b><i>ni</i></b>									
	3.46	2.32	L	5	+	-0.10				30	21
<i>Industrial/Traffic (MSY)</i>	2.08	1.01	L	7	**	-0.11				56	13

800  
801  
802  
803  
804  
805  
806  
807  
808  
809  
810  
811  
812  
813  
814  
815  
816  
817  
818  
819  
820  
821  
822  
823  
824  
825  
826  
827  
828  
829  
830  
831  
832

**Figure Captions:**

- Figure 1:** Location of the Barcelona (BCN) and Montseny (MSY) measuring stations. Red full circle highlights the location of the BCN measuring station before 2009. Green full circle highlights the new location of the BCN (from 2009) and MSY measuring stations.
- Figure 2:** Mann-Kendall fit of PM<sub>2.5</sub> trends at MSY station for the periods 2002-2010 (as in Cusack et al., 2012), 2004 – 2014 (this work), and 2002 – 2014 (largest period available in the time of writing). Reported are: magnitude of the trends [ $\mu\text{gm}^{-3}/\text{yr}$ ]; p-value; Total Reduction (TR) and Residual Component (RC). Significance of the trends following the Mann-Kendall test: \*\*\* (p-value < 0.001), \*\* (p-value < 0.01), \* (p-value < 0.05), + (p-value < 0.1).
- Figure 3:** Mann-Kendall (MK) and Multi-exponential (ME) trends for chemical species at BCN in PM<sub>10</sub>. Measured concentration (green line); Multi-exponential trend (red line); Multi-exponential residuals (blue line); Mann-Kendall trend (black line); Mann-Kendall residuals (grey line). Trend type: linear (L), single-exponential (SE), double exponential (DE).
- Figure 4:** Mann-Kendall (MK) and Multi-exponential (ME) trends for chemical species at MSY in PM<sub>10</sub>. Measured concentration (green line); Multi-exponential trend (red line); Multi-exponential residuals (blue line); Mann-Kendall trend (black line); Mann-Kendall residuals (grey line). Trend type: linear (L), single-exponential (SE), double exponential (DE).
- Figure 5:** Source contributions from PMF model in PM<sub>10</sub> at Montseny (MSY) and Barcelona (BCN). Mean values during 2004-2014. Values reported are: **Source**;  $\mu\text{g}/\text{m}^3$ ; %.
- Figure 6:** Mann-Kendall and Multi-exponential trends for source contributions in PM<sub>10</sub> at BCN. Measured concentration (green line); Multi-exponential trend (red line); Multi-exponential residuals (blue line); Mann-Kendall trend (black line); Mann-Kendall residuals (grey line). Trend type: linear (L), single-exponential (SE), double exponential (DE). Highlighted with yellow colour the source contributions at BCN from *Mineral*, *Traffic* and *Road/work resuspension* were excluded from the trend discussion.
- Figure 7:** Mann-Kendall and Multi-exponential trends for source contributions in PM<sub>10</sub> at MSY. Measured concentration (green line); Multi-exponential trend (red line); Multi-exponential residuals (blue line); Mann-Kendall trend (black line); Mann-Kendall residuals (grey line). Trend type: linear (L), single-exponential (SE), double exponential (DE).
- Figure 8:** Spanish national emission of SO<sub>2</sub> and NO<sub>x</sub> (normalized to year 2004).
- Figure 9:** NASA OMI level 3 tropospheric NO<sub>2</sub> column plotted using the Giovanni online data system, developed and maintained by the NASA GES DISC.
- Figure 10:** Annual (2004–2014) energy consumption for Spain (normalized to year 2004). Data from the Spanish Ministry of Industry (MINETUR, 2013).

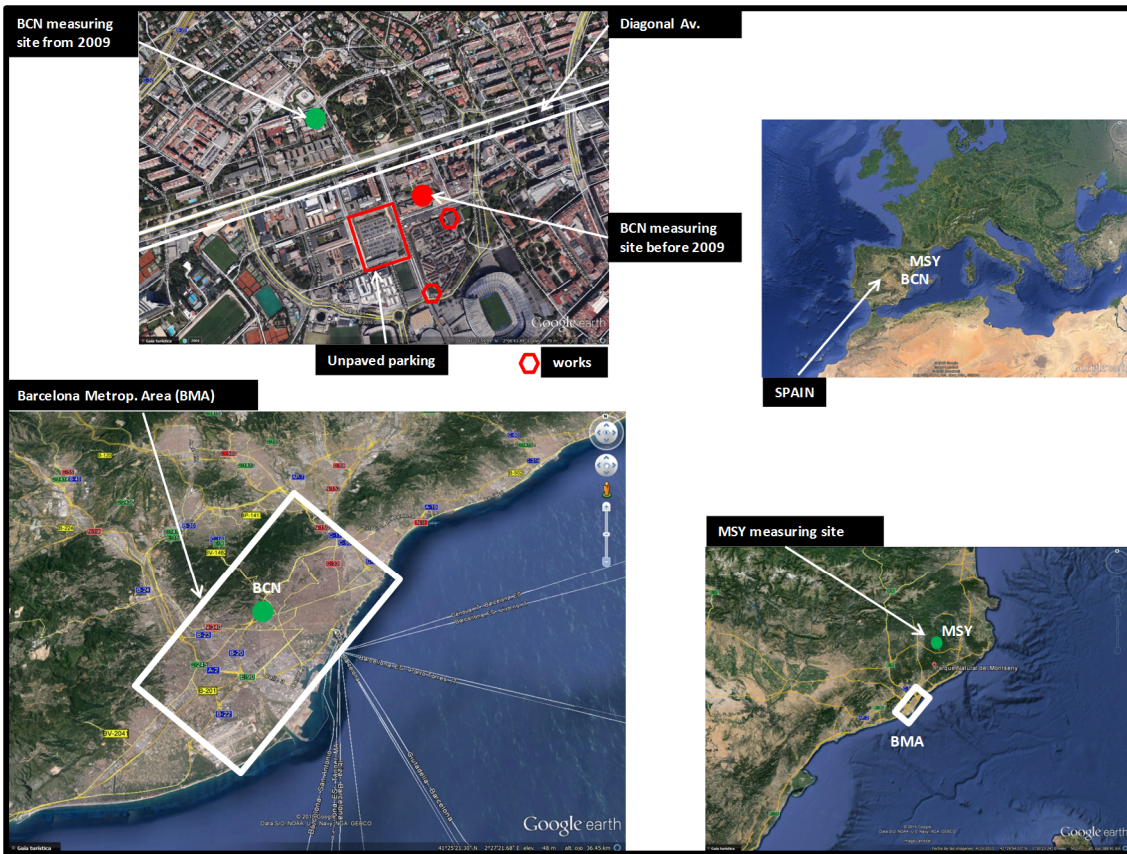


**Figure 1**

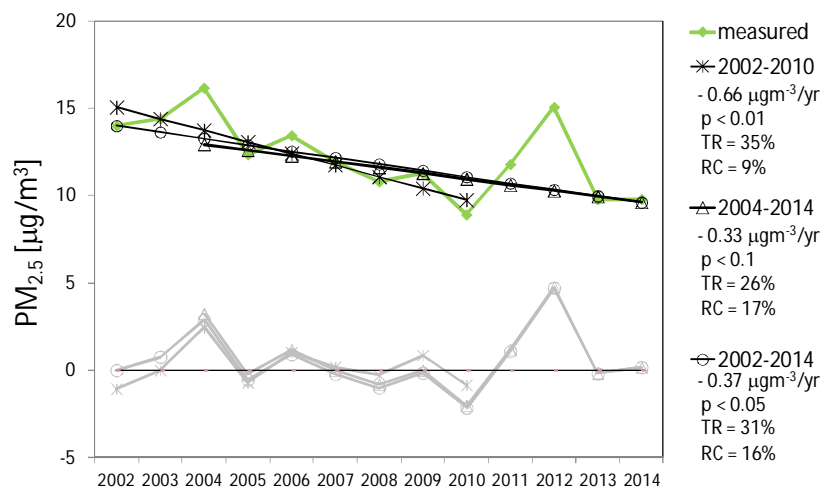


**Figure 2**

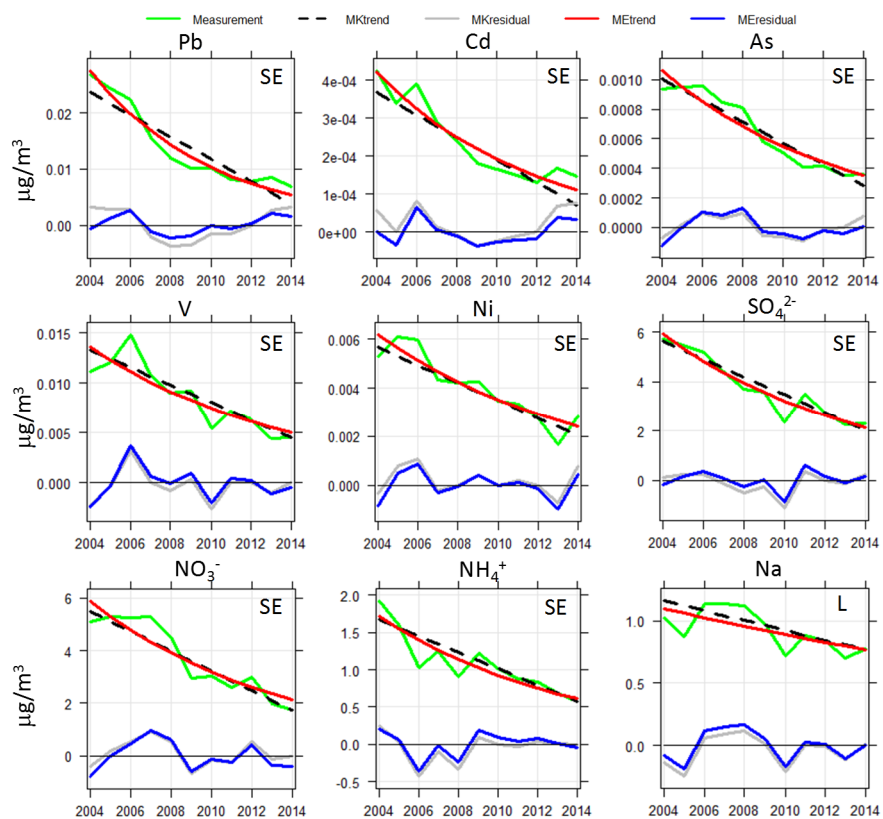


**Figure 3**

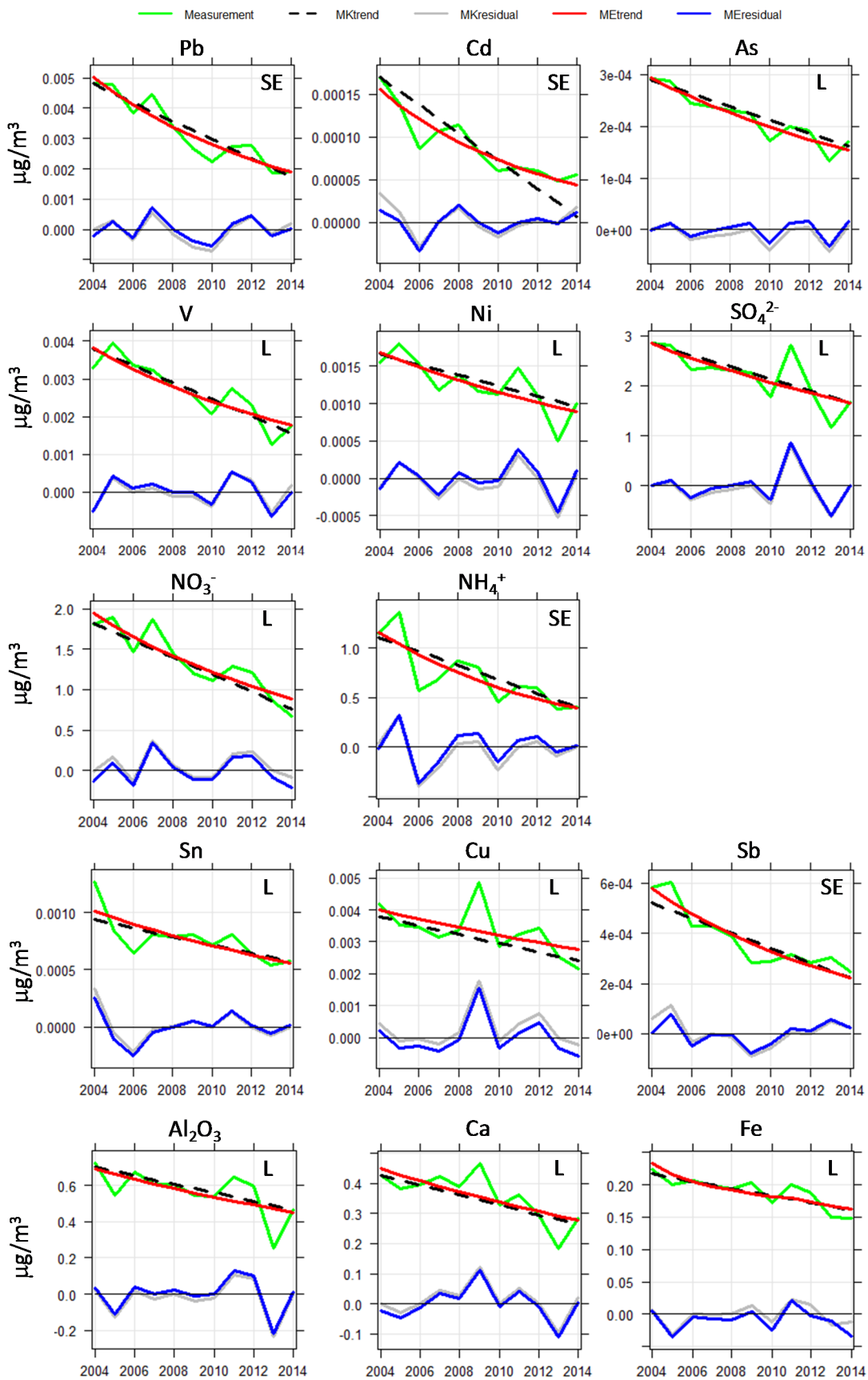


Figure 4

862

863

864

865

866

867

868

869

870

871

872

873

874

875

876

877

878

879

880

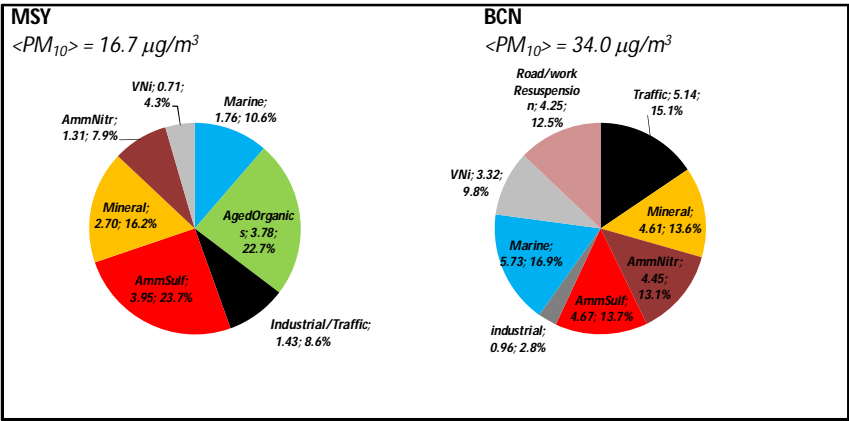


**Figure 5**



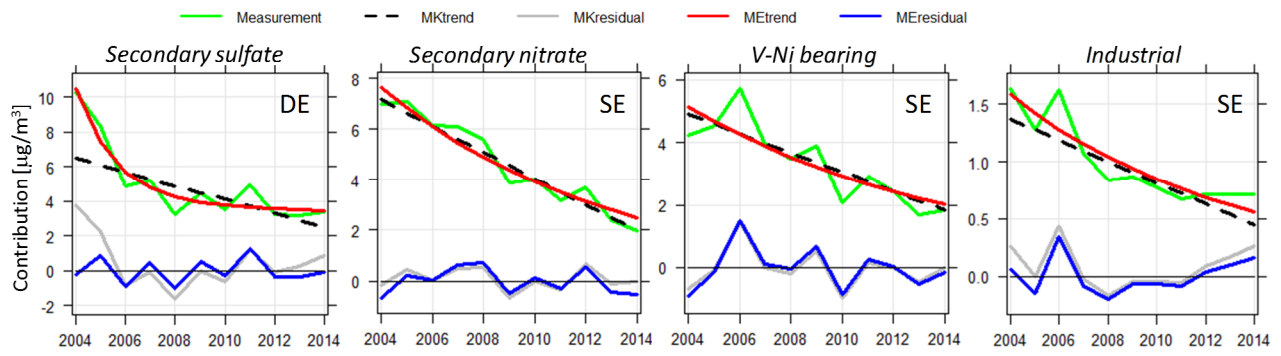


**Figure 6**

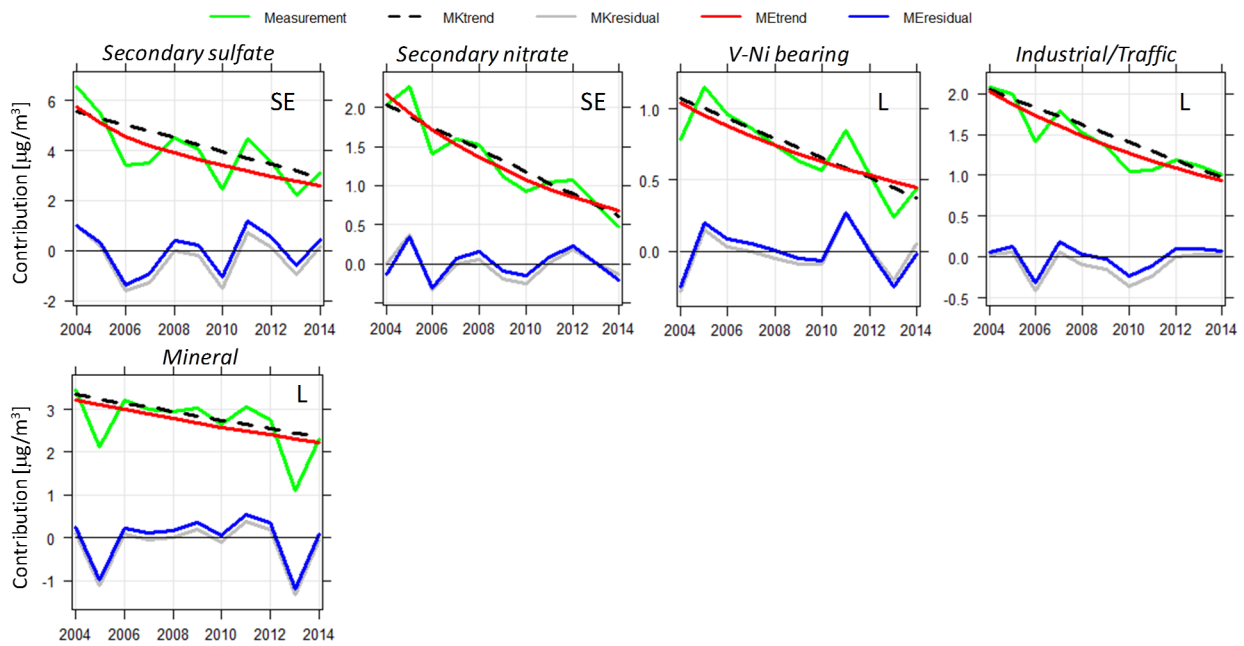
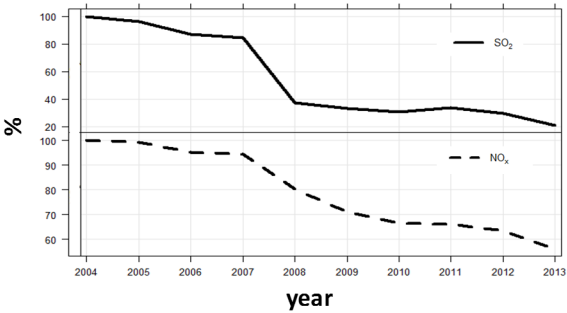


**Figure 7**

894

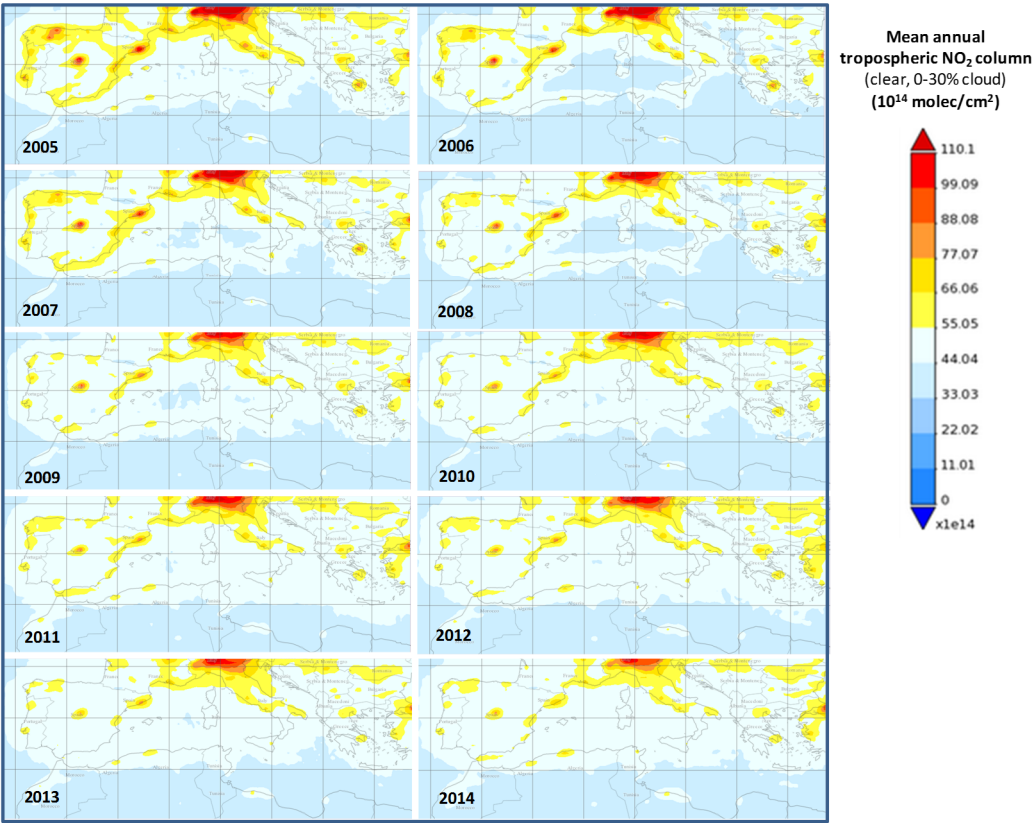


895

896 **Figure 8**

897

898



899

900 **Figure 9**

901

902

903

904

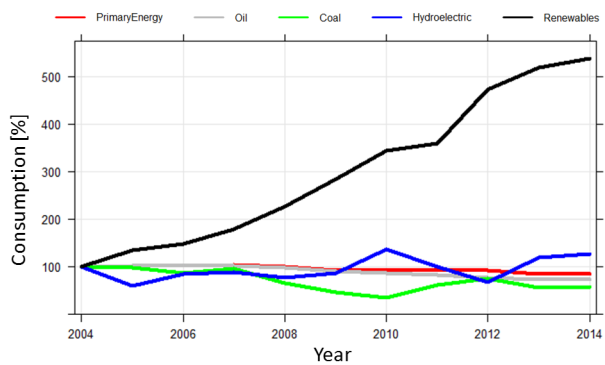


**Figure 10**